Journal of Medicinal Chemistry

Article

Discovery and profiling of a selective and efficacious Syk inhibitor

Gebhard Thoma, Alexander Baxter Smith, Maurice van Eis, Eric Vangrevelinghe, Joachim Blanz, Reiner Aichholz, Amanda Littlewood-Evans, Christian Lee, Hong Liu, and Hans-Guenter Zerwes

J. Med. Chem., **Just Accepted Manuscript** • Publication Date (Web): 29 Jan 2015

Discovery and profiling of a selective and efficacious Syk inhibitor

Gebhard Thoma,[a,*] Alexander B. Smith,[a] Maurice J. van Eis,[a] Eric Vangrevelinghe,[a] Joachim Blanz,[b] Reiner Aichholz,[b] Amanda Littlewood-Evans,[c] Christian C. Lee,[d] Hong Liu,[d] and Hans-Günter Zerwes[c]

[a]*Global Discovery Chemistry,* [b]*Analytical Sciences & Imaging,* [c]*Autoimmunity, Transplantation and Inflammation Research, Novartis Institutes for Biomedical Research, 4056 Basel, Switzerland;*

[d]*Genomics Institute of the Novartis Research Foundation, 10675 John Jay Hopkins Drive, San Diego, CA 92121, USA*

ABSTRACT: We describe the discovery of the selective and potent Syk inhibitor **11**, which exhibited favorable PK profiles in rat and dog and was found to be active in a collagen induced arthritis model in rats. Compound **11** was selected for further profiling but, unfortunately, in GLP toxicological studies it showed liver findings in rat and dog. Nevertheless, **11** could become a valuable tool compound to investigate the rich biology of Syk *in vitro* and *in vivo*.

INTRODUCTION

Spleen tyrosine kinase (Syk) is located in the cytoplasm of hematopoietic lineage cells except mature T cells. It plays a key role in mediating signal transduction *via* multiple receptors containing ITAM motifs (B-cell receptor in B-cells; Fc receptors in myeloid cells, basophils and mast cells; adhesion receptors; C-type lectin receptors). Following receptor stimulation, kinases of the src family phosphorylate tyrosine residues of the receptor intracellular ITAM domains, which serve as docking sites for the two SH2 domains of Syk. The kinase is recruited to the receptor and undergoes a conformational change leading to full catalytic activity. Syk phosphorylates various substrates (such as BLNK in B cells, SLP76 in myeloid cells, PLCγ2a, Vav, PI3-kinase family members, Cbl) and becomes part of a multi-protein signaling complex - the "signalosome" - leading to the activation of downstream effector pathways such as PKC, MAPK, NFκB.[1] Depending on the cell type and the triggers, effector functions such as proliferation, cytokine release and oxidative burst are initiated. These are the basis of physiological responses associated with (auto)immune, inflammatory or allergic reactions.

Blockade of the catalytic activity of Syk kinase is expected to abrogate these signaling pathways and to attenuate the biological responses. Thus, Syk is considered an attractive target for anti-inflammatory, anti-allergic and autoimmune diseases. In particular, prevention of activation of

cells *via* immune complexes or antigen triggering Fc receptor signaling and prevention of B cell receptor mediated events are believed to have therapeutic potential.[2] To probe this hypothesis in animals and in clinical trials, the availability of selective, drug-like Syk inhibitors is highly desirable.

Compounds targeting Syk were tested in a battery of assays. Potency and kinase selectivity were assessed in enzymatic assays based on the Caliper microfluidic mobility shift technology. Cellular activity was measured in Ramos B-cells upon BCR stimulation with anti-IgM which leads to phosphorylation of the adaptor protein BLNK (B cell linker protein), a direct Syk substrate. Inhibition of Syk in presence of 90% human blood was monitored in monocytes following FcγR stimulation with an anti CD32 antibody.[3] This leads to the phosphorylation of the adaptor protein SLP-76 which is also a direct substrate of Syk. To monitor cellular off-target inhibition (particularly Jak2) we used an assay measuring the IL3 dependent proliferation of mouse bone marrow cells.

Syk is an established target[3] first discovered in 1991.[4] Industry-wide efforts have been committed to identify selective antagonists[5] but, to our knowledge, BIIB-057 **1**[6] (Figure 1) is the only selective Syk inhibitor, which has been evaluated in clinical studies. However, a planned phase II trial in rheumatoid arthritis (RA) was withdrawn prior to patient enrollment.[7] The compound was potent in our enzymatic Syk assay (IC_{50} = 13 nM) and inhibited only 2 out of 77 additional kinases with IC_{50} values below 100 nM (ZAP70, 68 nM; PKCα, 90 nM; Table 1). Substantial activity was observed in the cellular Syk assay (IC_{50} = 178 nM). In human blood monocytes stimulated by activating CD32 in presence of blood Syk activity was inhibited with an IC_{50} value of ~1 μM. However, in both automated[8] and manual patch clamp assays[9] **1** significantly affected hERG channel activity with IC_{50} values around 10 μM.

Recently, Gilead disclosed the structure of GS-9973 **2**, which is being evaluated in cancer clinical trials.[10] Their compound was described as a highly potent and selective Syk inhibitor. However, in our assays **2** showed only modest activity particularly in the presence of blood (IC_{50} > 19 μM, Table 1). It is important to note that **2** considerably affected bone marrow cell proliferation which cannot be explained by Syk inhibition (Table 1).

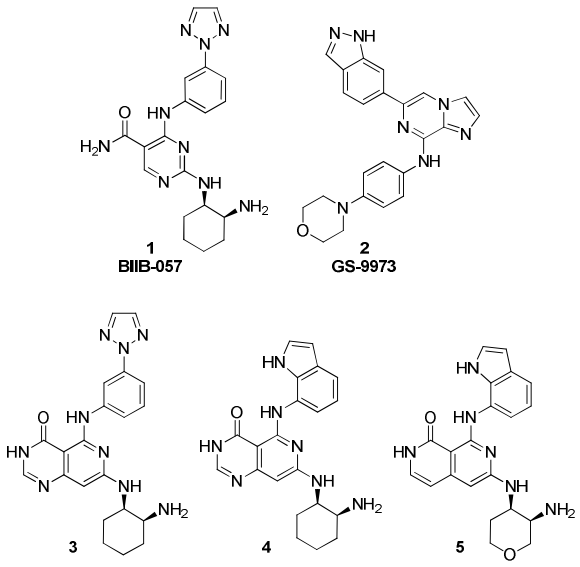

Figure 1. Structures of clinical compounds **1** and **2** as well as structures of reference compounds **3**, **4** and **5**

Table 1. Key *in vitro* data

Compound	Syk[a] (enzyme)	Kinase[b] selectivity	BM cell prolif.	Syk[a] (cell)	Syk[a] (blood)	hERG[a] Q-patch	hERG[c] man. patch
1	13 ± 4	2 (77)	5853	178 ± 8	952 ± 70	8600	42 % @ 10 µM 72 % @ 30 µM
2	377 ± 90	0 (58)	582	878 ± 88	19416 ±1474	n.d.	n.d.
3	5 ± 2	9 (36)	249	778 ± 132	n.d.	n.d.	n.d.
4	4 ± 0.6	3 (55)	3411	90 ± 15	307 ± 123	>30000	n.d.
5	22 ± 1	1 (55)	3515	55 ± 2	433 ± 159	24900	n.d.
6	19 ± 8	2 (59)	2601	445 ± 75	n.d.	8500	n.d.
7	165 ± 45	0 (59)	>10000	438 ± 34	n.d.	>30000	n.d.
8	1 ± 0.2	12 (67)	2110	69 ± 15	1788 ± 98	10000	n.d.
9	5 ± 1	4 (69)	5267	30 ± 2	302 ± 57	8100	13 % @ 3 µM 50 % @ 10 µM
10	5 ± 0.6	6 (64)	811	104 ± 29	274 ± 48	3700	n.d.
11	35 ± 4	0 (69)	9020	99 ± 7	367 ± 27	25900, >30000	0 % @ 10 µM 12 % @ 30 µM
12	1[d]	6 (58)	5270	14 ± 1	177 ± 53	3700	n.d.
13	94 ± 2	0 (67)	>10000	170 ± 54	782 ± 372	>30000	n.d.

[a] IC_{50} in nM; n ≥ 3 for Syk enzyme, cell and blood assays (SEM shown).

[b] number of kinases with IC_{50} < 100 nM in addition to Syk (number of kinases tested).

[c] inhibition at indicated concentration; 3 independent measurements for each concentration

[d] tested once

In a previous communication we reported a series of napthyridinone and pyridopyrimidinone Syk inhibitors with bicyclic cores sharing the binding mode of compound **1**.[11] Initial compounds such as **3** containing substituted anilines displayed poor kinase selectivity and moderate cellular activity (IC_{50} = 778 nM, Table 1). In contrast, replacement of aniline with a 7-aminoindole substituent led to compounds such as **4** and **5** with acceptable kinase selectivity, good cellular activity (IC_{50} < 100 nM), high potency in the presence of blood (IC_{50} < 500 nM) and little or no hERG channel inhibition (Table 1). Unfortunately, we failed to improve the poor PK properties of these compounds and, consequently, these series were abandoned. In efforts to overcome these PK liabilities, we investigated monocyclic analogs of **1** based on pyridine (**6**, **7**), pyrazine (**8**, **9**), triazine (**10**, **11**, **12**) and pyrimidine cores (**13**).

Here we describe discovery and profiling of the potent, highly selective and orally bioavailable Syk inhibitor **11**, which shares the binding mode of **1**, **3**, **4** and **5**.

CHEMISTRY

The pyridine derivative **6** was prepared from building block **14** (Scheme 1). The reaction with aniline **15** led to **16**. Compound **15** was treated with an excess of LiHMDS (3 eq.) prior to the addition of acid **14** to obtain the desired regioisomer **16** in good yield. Compound **16** was transformed into the methyl ester **17**. The Boc-protected diaminocyclohexane **18** was introduced giving **19**, which was converted into amide **20**. Removal of the protecting group afforded compound **6**.

Scheme 1. Synthesis of compound **6**[a]

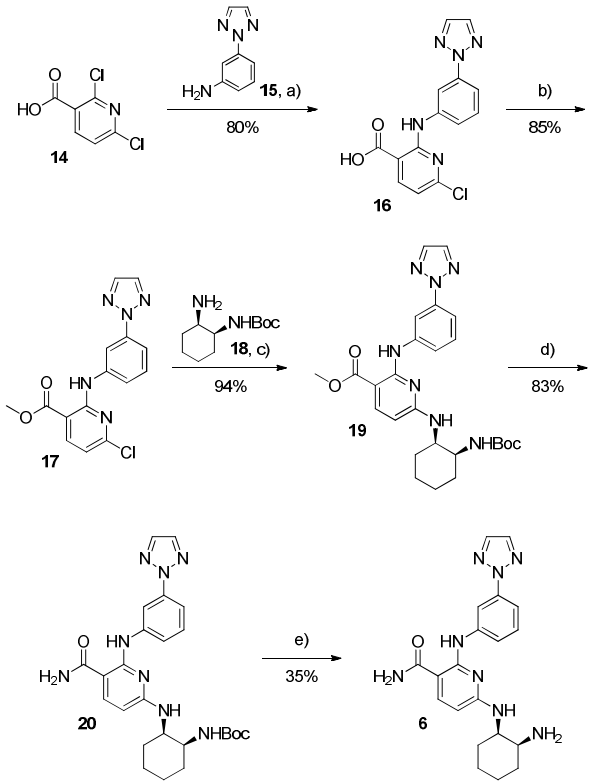

[a] Reagents and conditions: (a) (1) **15**, LiHMDS, THF, 1 h, -78^{0}C, (2) add **14**, -78→25^{0}C, 1 h, (b) (1) CDI, DMF, 16 h, 25^{0}C, (2) add MeOH, 0.5 h, 25^{0}C, (c) **18**, DIPEA, NMP, 16 h, 120^{0}C, (d)

(1) LiOH, H_2O, dioxane, 2 h, 100^{0}C, (2) COMU, DIPEA, DMF, NH_4OH, 1 h, 25^{0}C, (e) TFA, CH_2Cl_2, 1 h, 25^{0}C.

Compound **7** was accessible from building block **21** (Scheme 2). The Boc-protected diaminocyclohexane **18** was introduced to give **22**. Palladium catalyzed coupling with aminoindole **23** led to **24** which was transformed into amide **25**. Deprotection afforded compound **7**.

Scheme 2. Synthesis of compound **7**[a]

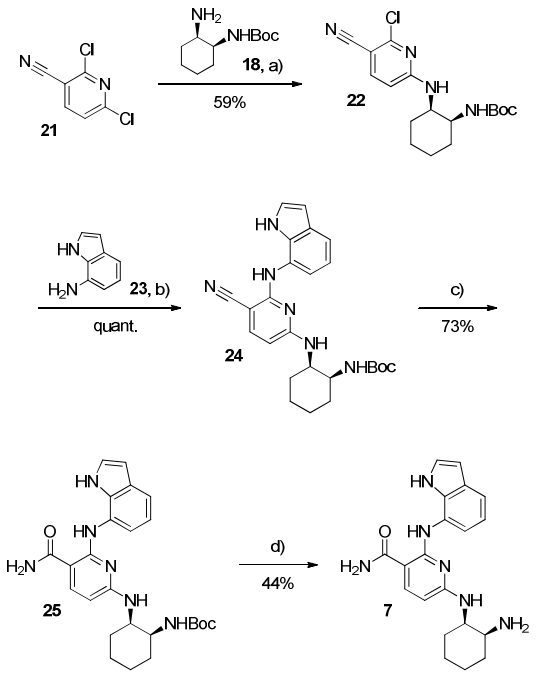

[a] Reagents and conditions: (a) **18**, NMP, NEt_3, 16 h, 75^{0}C, (b) **23**, $Pd(OAc)_2$, Xantphos, K_2CO_3, dioxane, 1.5 h, 150^{0}C, (c) H_2O_2, NaOH, DMSO, EtOH, 3 h, 25^{0}C, (d) HCl, CH_2Cl_2, 2 h, 0→25^{0}C.

Pyrazine **8** was obtained from building block **26**, which was reacted with the Boc-protected diaminocyclohexane **18** to give **27** (Scheme 3). The regioisomer of **27** was also isolated (19%). Introduction of aniline **15** led to **28**, which was transformed into amide **29**. Deprotection afforded compound **8**.

Scheme 3. Synthesis of compound **8**[a]

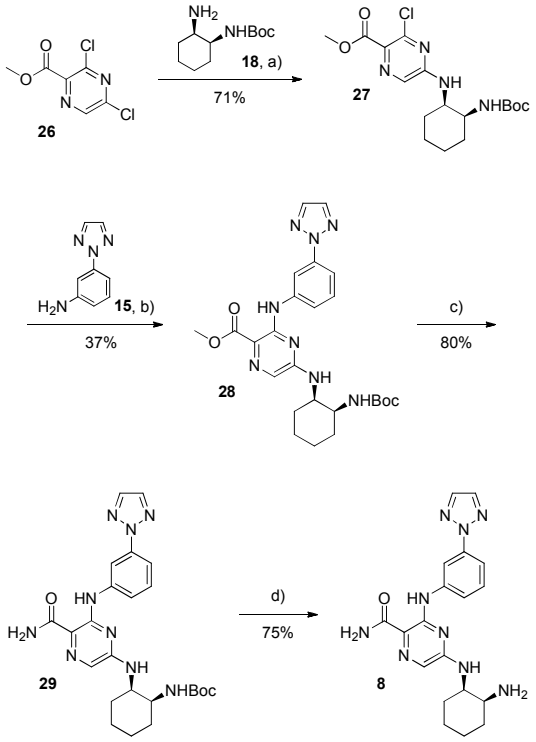

[a] Reagents and conditions: (a) **18**, DMF, NEt_3, 16 h, 0→25^{0}C, (b) **15**, $Pd(OAc)_2$, Xantphos, K_2CO_3, dioxane, 16 h, 90^{0}C, (c) (1) LiOH, H_2O, dioxane, 2 h, 25^{0}C, (2) COMU, DIPEA, DMF, NH_4OH, 0.5 h, 25^{0}C, (d) HCl, CH_2Cl_2, MeOH, 16 h, 25^{0}C.

Indole derivative **9** was obtained from building block **30** which was reacted with the Boc-protected diaminocyclohexane **18** to give **31** (Scheme 4). Introduction of aminoindole **23** led to **32** which was transformed into amide **33**. Deprotection led to compound **9**.

Scheme 4. Synthesis of compound **9**[a]

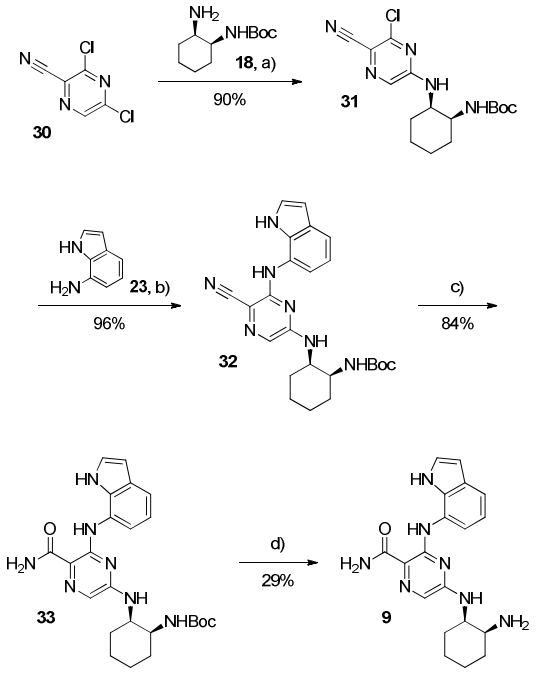

[a] Reagents and conditions: (a) **18**, DMF, NEt_3, 16 h, 0→25^{0}C, (b) **23**, $Pd(OAc)_2$, Xantphos, K_2CO_3, dioxane, 16 h, 90^{0}C, (c) H_2O_2, NaOH, DMSO, EtOH, 2 h, 0→25^{0}C, (d) HCl, CH_2Cl_2, MeOH, 16 h, 25^{0}C.

Triazine **10** was prepared from building block **34** which was reacted with aniline **15** to give **35** (Scheme 5). Compound **35** was transformed into amide **36**. Oxidation of **36** with *m*-CPBA led to the formation of a mixture of sulfoxide and sulfone, which was treated with the Boc-protected diaminocyclohexane **18** to give **37**. Deprotected afforded compound **10**.

Scheme 5. Synthesis of compound **10**[a]

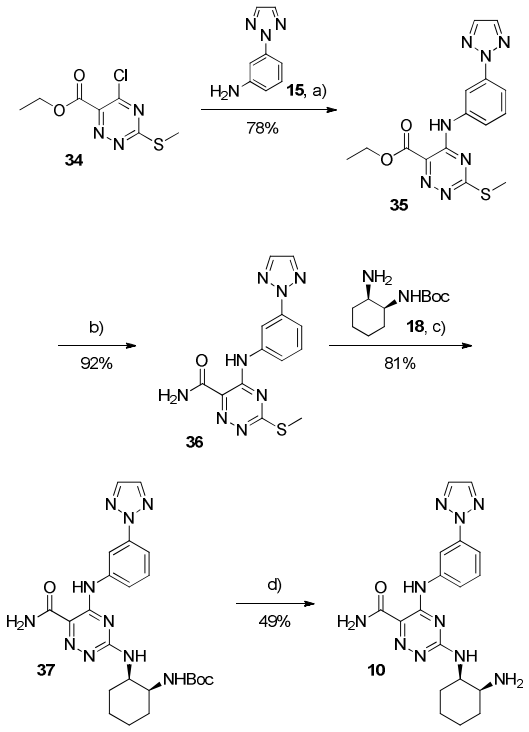

[a] Reagents and conditions: (a) **15**, NMP, 0.5 h, 0→25^{0}C, (b) NH_3 (7M) in MeOH, 2 h, 25^{0}C, (c) (1) *m*-CPBA, DMF, 2 h, 0→45^{0}C, (2) **18**, NEt_3, 2 h, 25→65^{0}C, (d) TFA, CH_2Cl_2, 1 h, 25^{0}C.

Indole derivative **11** was also prepared from building block **34** (Scheme 6). The introduction of 7-aminoindole **23** led to **38**. The indole was protected to give **39**, which was transformed into amide **40**. The sulfur atom of compound **40** was oxidized leading to a mixture of sulfoxide and sulfone. Susequent treatment with the Boc-protected diaminocyclohexane **18** gave **41**. Deprotection furnished compound **11**. The deprotection had to be carefully monitored because of the formation of side products, which were difficult to separate (probably dimerization of the indole due to the acidic reaction conditions). Compound **12** was prepared following analogous procedures but using 4-aminoindole instead of 7-aminoindole (see experimental section).

Scheme 6. Synthesis of compound **11** and **12**[a]

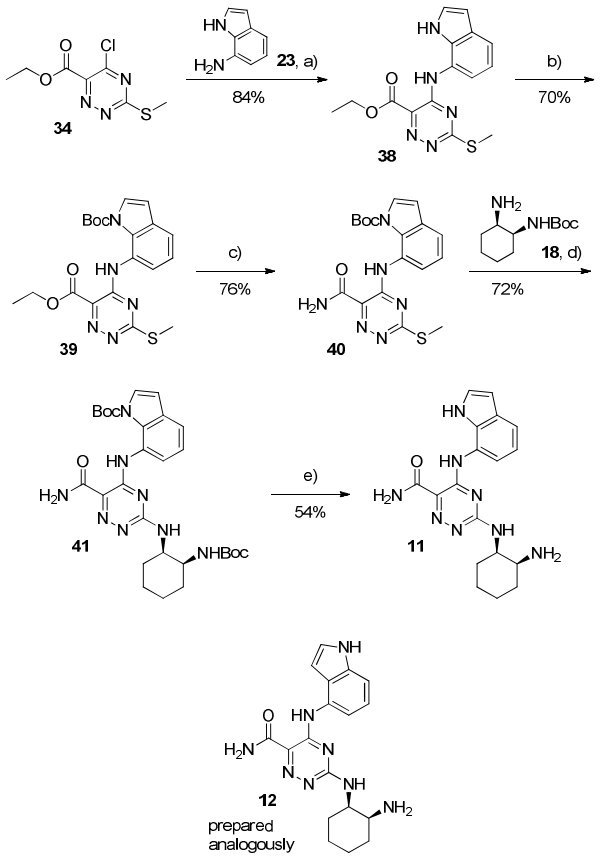

[a] Reagents and conditions: (a) **23**, NMP, 0.25 h, 25^{0}C, (b) DMAP, $(Boc)_2O$, THF, 0.5 h, 0→25^{0}C, (c) NH_3 (7M) in MeOH, 0.75 h, 25^{0}C, (d) (1) *m*-CPBA, DMF, 0.75 h, 0^{0}C, (2) **18**, NEt_3, 0.25 h, 65^{0}C, (e) TFA, H_2O, CH_2Cl_2, 17.5 h, 0→25^{0}C.

Pyrimidine **13** was prepared from building block **42**, which was reacted with aminoindole **23** to give **43**. Introduction of benzyloxycarbonyl-protected diaminocyclohexane **44** led to **45**, which was deprotected to afford compound **13**. The benzyloxycarbonyl-protected building block **44** was used to avoid acidic deprotection conditions, which led to side product formation in the synthesis of compound **11**.

Scheme 7. Synthesis of compound **13**[a]

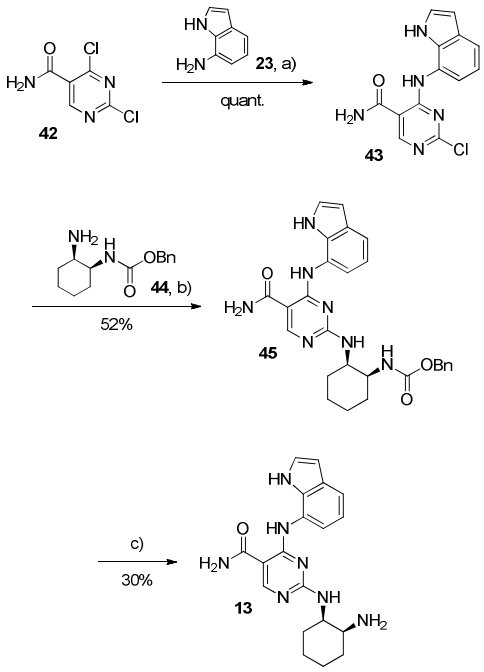

[a] Reagents and conditions: (a) **22**, THF, NEt_3, 16 h, 25^{0}C, (b) **44**, DMF, NEt_3, 3 h, 110^{0}C, (c) Pd/C, H_2, MeOH, 3.5 h, 25^{0}C.

RESULTS AND DISCUSSION

Compounds **6-13** were broadly assessed and compared to competitor compound **1** (Table 1). In the enzymatic Syk assay the triazolyl-anilines **1**, **6**, **8** and **10** (IC_{50} values of 13, 19, 1 and 5 nM, respectively) were generally found to be more potent than the corresponding 7-aminoindoles **13**, **7**, **9** and **11** (IC_{50} values of 94, 165, 5 and 35 nM, respectively). However, in the cellular Syk assay compound pairs with the same core structure showed similar potency (pyrimidines **1** and **13**, 178 and 170 nM; pyridines **6** and **7**, 445 and 438 nM; pyrazines **8** and **9**, 69 and 30 nM; triazines **10** and **11**, 104 and 99 nM). With the exception of pyridines **6** and **7** all new compounds **8**-**13** were at least equipotent to **1**. As we had observed previously for related bicyclic compounds **3**, **4**, and **5**[11] (Table 1) the 7-aminoindoles **13**, **7**, **9** and **11** were found to be more selective in our enzymatic kinase panel than the corresponding triazolyl-anilines **1**, **6**, **8** and **10**. The inferior selectivity of the triazolyl-anilines compared to the 7-aminoindoles was confirmed by more pronounced effects in the bone marrow cell proliferation assay, which is independent of Syk (Table 1). The 4-aminoindole **12** was found to be the most potent compound with IC_{50} values of 1 and 14 nM in the enzymatic and cellular assays, respectively. Unfortunately, **12** showed limited selectivity inhibiting 6 out of 58 kinases with IC_{50} values below 100 nM but did not significantly affect bone marrow cell proliferation (IC_{50} > 5 μM). We previously had observed the reduced kinase selectivity of 4-aminoindole derivatives with bicyclic cores sharing the binding mode of the compounds discussed here.[11]

To understand the superior kinase selectivity of the 7-aminoindoles we compared the high resolution X-ray co-structures of compounds **10** and **11** bound to Syk catalytic domain.[12] Both the triazolyl-aniline **10** and the corresponding indole **11** form two strong hydrogen bonds with the hinge sequence of Syk (E449, A451; Figure 2). Both the aniline of **10** and the indole of **11** are sandwiched between the side chain of L377 and P455 located at the proximal P-loop and downstream hinge regions, respectively. However, the orientation of the aromatic substituents differs. The N-linked triazole of **10** is oriented toward the diaminocyclohexane whereas the 5-membered ring of the indole of **11** is directed toward the downstream hinge region of Syk. Overall, the bioactive (bound) conformation of aniline **10** is more compact compared to **11**. The indole of **11** can form an additional H-bond with A451 **11**. However, this H-bond is most likely weak as the carbonyl oxygen of A451and the nitrogen of the indole are not optimally positioned. The weakness of the hydrogen bond is supported by the slightly inferior activity of the 7-aminoindoles in the biochemical assay. As we did not attempt to co-crystallize our compounds with other kinases, the rationale for the superior selectivity of the 7-aminoindoles remained elusive.

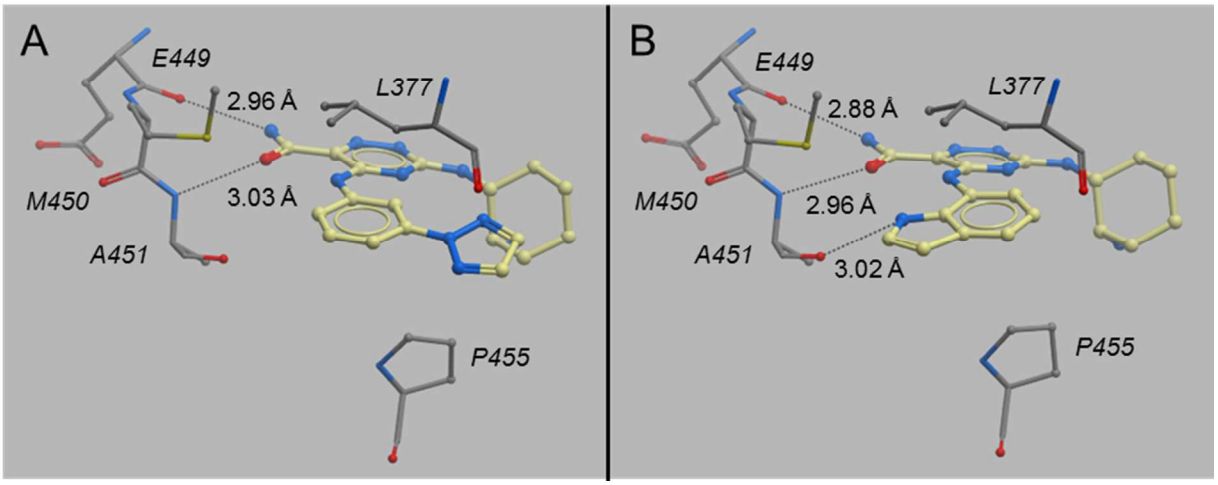

Figure 2. Crystal structures of triazines **10** (A) and **11** (B) bound to the kinase domain of Syk

Pyrimidine **1** and pyridine **6** showed superior kinase selectivity compared to pyrazine **8** and triazine **10**. In contrast to **1** and **6**, compounds **10** and **8** can form an intramolecular H-bond between the amide NH and the triazine core, which is expected to reduce the rotation of the amide out of the plane of the aromatic ring (Figure 3A). This assumption was supported by DFT/B3LYP calculations in the gas phase[12] indicating a more pronounced distortion of the amide for **1** compared to **10** with dihedral angles of 16^0 and 2^0, obtained for the respective optimized geometries (Figure 3B). As compound **3** with a perfectly planar bicyclic pyridopyrimidinone core, which shares the binding mode of compounds **1**, **6**, **8** and **10** also showed limited kinase selectivity (Table 1)[11], we speculated that a distortion of the hinge-binding amide motif improves the kinase selectivity of compounds with this binding mode. However, when we analyzed the structures of pyrimidine **1** and triazine **10** bound to Syk catalytic domain we learned that the bound conformations superimposed almost perfectly and showed very small distortions of the amide with similar dihedral angles of ~8^o and ~4^o for **1** and **10**, respectively.

Pyrazines **8** and **9** as well as triazines **10** and **11** which form an intramolecular H-bond (flat core) were more potent but less selective than the corresponding pyridines **6** and **7** or pyrimidines **1** and **13** which do not form an intramolecular H-bond (Table 1). Thus, compounds **9** and **11** combining a 7-aminoindole substituent (inducing selectivity) and a "flat" core (inducing potency) were considered most promising.

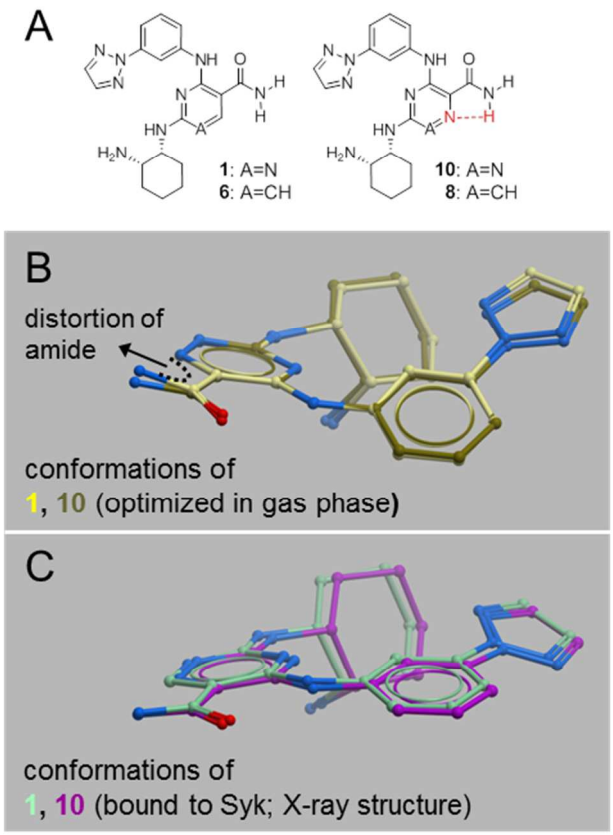

Figure 3. A) Compounds **10** and **8** can form an intramolecular H-bond, compounds **1** and **6** cannot. Thus, an increased distortion of the amide is expected for **1** and **6**. B) DFT/B3LYP calculations in the gas phase[12] indicate a more pronounced distortion of the amide for **1** compared to **10** with dihedral angles of 16^0 and 2^0, measured for the respective optimized geometries. C) The conformations of compounds **1** and **10** bound to the Syk catalytic domain superimpose almost perfectly and show very small distortions of the amide with similar dihedral angles of ~8° and ~4° for **1** and **10**, respectively. For simplicity, the amino acids of the protein are omitted.

Compounds **8**, **9**, **10**, **11**, **12** and **13** were tested for Syk inhibition in whole blood monocytes (IC_{50} values of 1788, 302, 274, 367, 177 and 782 nM, respectively) and – with the exception of **8** – were found to be superior to **1** (IC_{50} = 952 nM). Interestingly, compared to the 7-aminoindole

11, the corresponding 4-aminoindole **13** was only 2 fold more potent in the blood assay despite of its clearly superior potencies in both enzymatic and cellular assays (35-fold and 7-fold, respectively. Inhibition of the hERG channel was assessed in an automated patch clamp assay (Q-patch, Table 1).[8] The 7-aminoindoles **13**, **7** and **11** showed reduced effects (IC_{50} > 20 μM) compared to their triazolyl-aniline analogs **1**, **6** and **10** (IC_{50} < 10 μM). The pyrazines **8** and **9** showed similar IC_{50} values (~ 10 μM). The 4-aminoindole **12** significantly inhibited hERG channel activity with an IC_{50} value of 3.7 μM. Compounds **9** and **11** were also tested in a manual patch clamp assay.[9] Pyrazine **9** considerably inhibited the hERG channel activity (50% at 10 μM) whereas triazine **11** did not show any inhibition at 10 μM and only 12 % inhibition at 30 μM and, thus, differentiated favorably from compound **1**.

Compounds **9** and **11** showed favorable PK properties in rat (Table 2). Medium clearance (CL) and high volume of distribution (V_{SS}) led to long mean residence times (MRT). Both exposure (AUC) and oral bioavailability (BAV) were acceptable. Slow absorption led to flat PK curves avoiding high peak concentrations (Figure 4). In dogs, compound **11** also showed good exposure, acceptable oral bioavailability and a long MRT (Table 2). The corresponding 4-aminoindole **12** showed very limited exposure, higher clearance and a shorter MRT.[13] Due to the poor PK properties, the hERG channel inhibition and limited selectivity the slightly more potent compound **12** was not further considered (2-fold more potent than **9** and **11** in the most relevant whole blood assay, Table 1).

Table 2. PK data on compounds **9**, **11** and **12**

Parameter	**9**	**11**		**12**
species	rat[a]	rat[a]	dog[b]	rat[a]
CL (mL min^{-1} kg^{-1})	28	31	11	83
V_{SS} (L/kg)	12.3	16.4	6.8	10.3
MRT (h)	7.2	8.7	8.4	2.1
AUC iv[c] (nM h)	1'610	1'459	3414	522
AUC po[c] (nM h)	1'523	877	1836	19
BAV (%)	95	60	54	4
C_{max}[c] (nM)	108	80	139	4

[a] Cassette dosing in Sprague Dawley rats; i.v. 1 mg/kg, NMP:PEG200 (3:7); p.o. 3 mg/kg, CMC:water:tween (0.5:99:0.5).

[b] One in one dosing in Beagle dogs; i.v. 0.1 mg/kg, NMP:PEG200 (3:7); p.o. 0.3 mg/kg, MC:water (0.5:99.5).

[c] dose normalized.

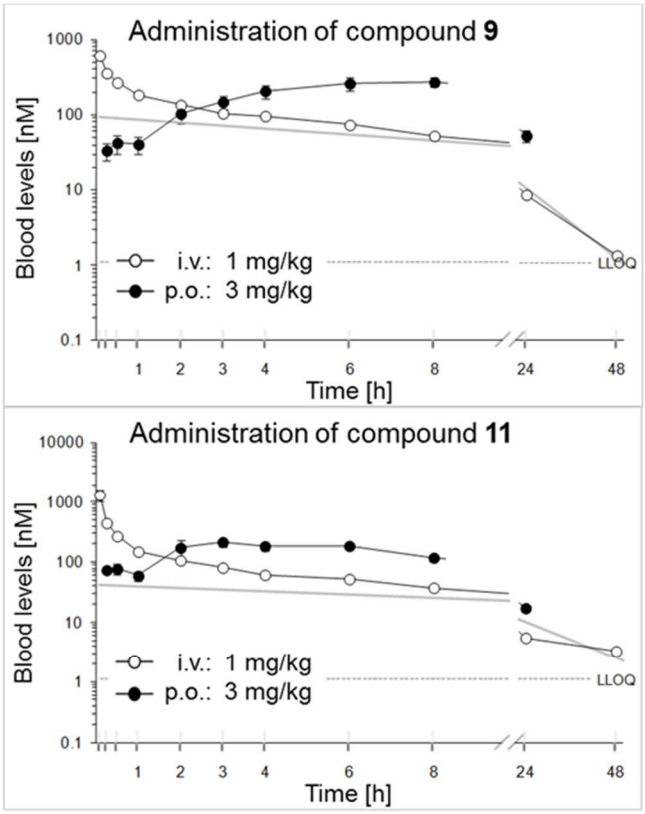

Figure 4. PK curves for **9** and **11** following i.v. and p.o. dosing in rat

Compound **11** was selected for further profiling. For a broader exploration of the kinase selectivity, the binding of **11** to a panel of 451 kinases was assessed (Figure 5).[14] Only 14 of the kinases demonstrated remarkable binding affinity to **11** and K_d-values were determined. Compound **11** was found to bind most strongly to Syk (K_d = 0.64 nM) exhibiting 20-fold selectivity over Pak7, 25-fold selectivity over Pak4 and ≥100-fold selectivity over the remaining kinases. The K_d for Zap70 which is the closest analog of Syk was 65 nM resulting in a selectivity factor of 100. In the biochemical Caliper assays, we observed only a 7-fold selectivity over Zap70 (Table 3). However, in a cellular assay interrogating Zap70 activity (antiCD3-induced Zap70-dependent phosphorylation of SLP76 in Jurkat cells), compound **11** was found to be 25-fold less potent than in a similar assay interrogating Syk activity (anti IgM-induced BLNK

phosphorylation; Table 3). Compound **1** showed only 10-fold selectivity in this most relevant cellular assay. Overall, compound **11** exhibited a very promising kinase selectivity profile to warrant further experiments.

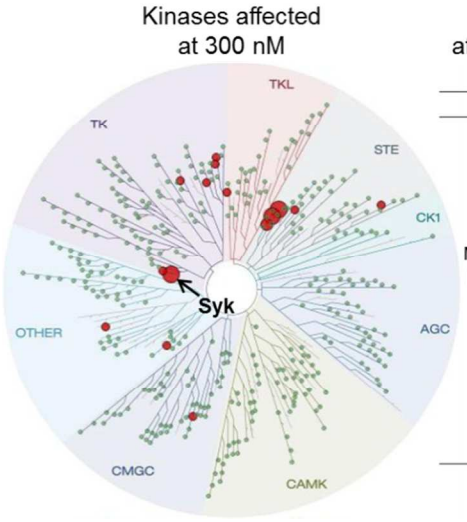

K_d values on affected kinases

Kinase	K_d [nM]
AXL	71
BUB1	240
GCN2	150
IRAK1	67
JAK2	53
MAP3K2	140
MERTK	150
PAK4	17
PAK6	110
PAK7	12
ROS1	120
SLK	380
SYK	0.64
ZAP70	65

Figure 5. Kinase selectivity profile of compound **11**. In addition to Syk only 13 out of 451 kinases were affected at a concentration of 300 nM. For these kinases K_d values were determined.

Table 3. Selectivity of compound **11** over Zap70

Assay [nM]	**1**	**11**
Syk (enzyme)	13 ± 4	35 ± 4
Syk (K_d)	n.d.	0.64
Syk (cell)	178 ± 8	99 ± 7
Zap70 (enzyme)	76 ± 13	251 ± 23
Zap70 (K_d)	n.d.	65
Zap70 (cell)	1805 ± 305	2526 ± 493

We established a rat PK/PD model in which compound **11** was administered to Lewis rats (Figure 4). Blood samples were taken at different times post dosing for PK determinations as well as assessment of inhibition of Syk-dependent signaling events. For this, the extent of SLP76 phosphorylation in monocytes in response to stimulation by anti CD32 was quantified. A representative experiment is shown in Figure 6A. A dose of 22 mg/kg of **11** led to 90, 85 and 45 % inhibition after 2, 4 and 24 h post administration, respectively. Blood concentrations were 900, 1100 and 300 nM, respectively. Analysis of individual samples from several experiments involving different doses (30 - 3 mg/kg) and time points (2, 4, 24 h) indicated a dose and exposure-dependent inhibition of the PD response *ex vivo* (FcgR-induced P-SLP76 in peripheral blood monocytes) with blood IC_{50} levels of 189 nM (Figure 6B).

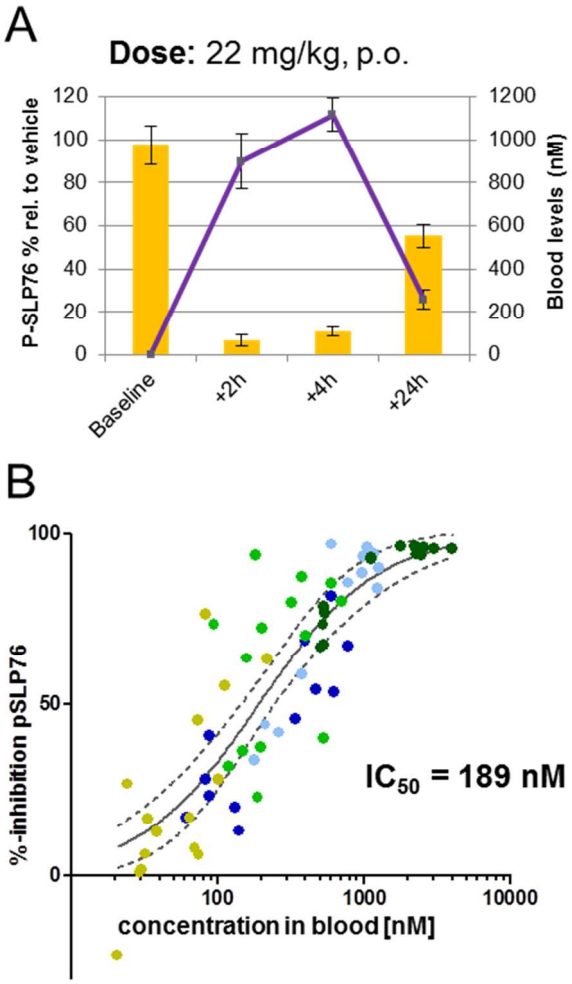

Figure 6. PK/PD experiments with compound **11**. (A) Single dose treatment of Lewis rats followed by ex-vivo assessment of blood compound levels (PK) and FcgR-induced P-SLP76 in peripheral blood monocytes (PD). (B) The IC_{50} value was determined by PK/PD analysis of individual samples from several experiments involving several doses (30 - 3 mg/kg) as well as several time points (2, 4, 24 h). The colors indicate data from distinct dosing groups (dark green: 30 mg/kg; light blue: 22 mg/kg; light green and dark blue: 10 mg/kg; yellow: 3 mg/kg).

Efficacy of **11** was demonstrated *in vivo* in a rat collagen-induced arthritis model in which the compound dosing was started when rats developed paw swelling (day 15) subsequent to immunization (day 0) and boost (day 7) with porcine collagen.[15] In this "therapeutic" model compound **11** showed rapid and sustained reversal of paw swelling at 10 and 30 mg/kg p.o. q.d. and inhibition of swelling at 3 mg/kg p.o. q.d. with slow onset but significant inhibition vs. placebo (Figure 7A). The treated animals displayed higher body weight gain compared to vehicle-treated animals due to reduced joint swelling and good tolerability of compound **11** (Figure 7B). The reversal of joint swelling was also reflected in improved histology (reduced inflammation and cartilage and proteoglycan loss; Figure 7C). Peak compound concentrations in the blood of treated animals were 126 nM, 866 nM and 2891 nM for the doses of 3, 10 and 30 mg/kg, respectively (Figure 7D). It is worthwhile to mention that a statistically significant reduction of joint swelling (3 mg/kg dose) was observed at exposure levels below the IC_{50} value of 189 nM determined for **11** in the PK/PD model.

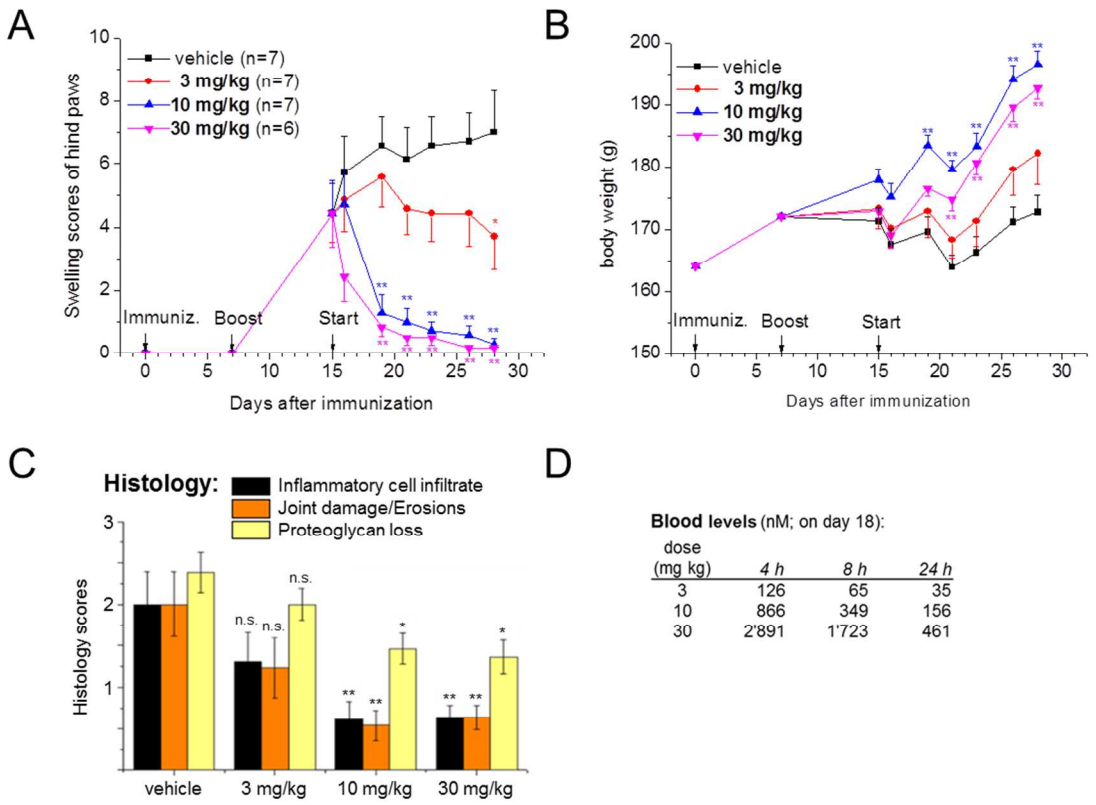

Figure 7. Inhibition of collagen-induced arthritis in female Lewis rats by compound **11**. (A) Rats were immunized on day 1 with collagen and boosted after 7 days. Joint swelling developed in hind paws. Rats with swollen joints were randomized to treatment groups. Compound **11** was administered once daily at the indicated doses. (B) Body weight of treated and untreated rats. (C) Histology scores for inflammation, bone and cartilage damage in hind paws at termination of the experiment on day 28 (D) Blood levels of compound **11** for all doses were determined on day 18 (3rd day of treatment) at the indicated time points.

Because of its favorable profile compound **11** was investigated in toxicology studies in rats and dogs. Unfortunately, in 4 weeks GLP studies we observed liver findings such as single necrosis of hepatocytes, bile plugs and portal inflammation. Furthermore, in the GLP *in vitro* hERG assay, compound **11** showed an IC_{50}-value of 5 µM, which was unexpected considering the non-GLP

data (Table 1). However, in a dog telemetry study no prolongation of the QT interval was observed. Compound **11** was nonetheless abandoned mainly because of an insufficient therapeutic index for autoimmune indications.

As Syk expression is limited to hematopoietic lineage cells[1], we attributed the liver findings to the chemical structure of **11** but not to its mode of action. Studies of the metabolism of **11** *in vitro* (liver microsomes) and *in vivo* (rat) did not indicate the presence of reactive metabolites. However, experiments with radiolabeled **11** in hepatocytes pointed to covalent adduct formation. Furthermore, incubation of **11** with hepatocytes afforded cysteine conjugate **46** (Figure 8A) which possibly originated from a reactive metabolite trapped by glutathione or cysteine. To the best of our knowledge, the formation of a cysteine adduct such as **46** is unprecedented. Metabolite **46** (0.9 μg) was isolated from incubation of parent compound **11** with monkey liver slices. The structure was assigned by NMR based on the following observations (Figure 8B): (a) The spin system H-4, H-5, H-6 was observed by TOCSY (total correlation spectroscopy) indicating that there was no additional substitution compared to **11**. (b) A proton of the indole nitrogen (N-1) was not observed. (c) The signal for H-4 was shifted to 8.31 ppm (7.44 ppm in **11**, Figure 8C) which is in line with a de-shielding effect of the carbonyl function at C-3. (d) A single proton at the nitrogen (N-18) of the cysteine was detected and the chemical shift of 4.12 ppm for H-19 indicated an N-linked cysteine. Additional evidence came from MS experiments (Figure 8D). Collision-induced dissociation of the protonated molecular ion of **46** (m/z=500) resulted in the loss of CO_2 (m/z=456) followed by the loss of hydrogen sulfide (m/z=422). The loss of hydrogen sulfide can only occur if the cysteine is linked to the indole *via* nitrogen but not if it is linked *via* sulfur. The elemental formula of **46** and the fragment ions was supported by accurate

mass measurements. The metabolic pathway leading to **46**, the structure of the primary metabolite, as well as the contribution of this metabolite to the observed liver findings, remains elusive.

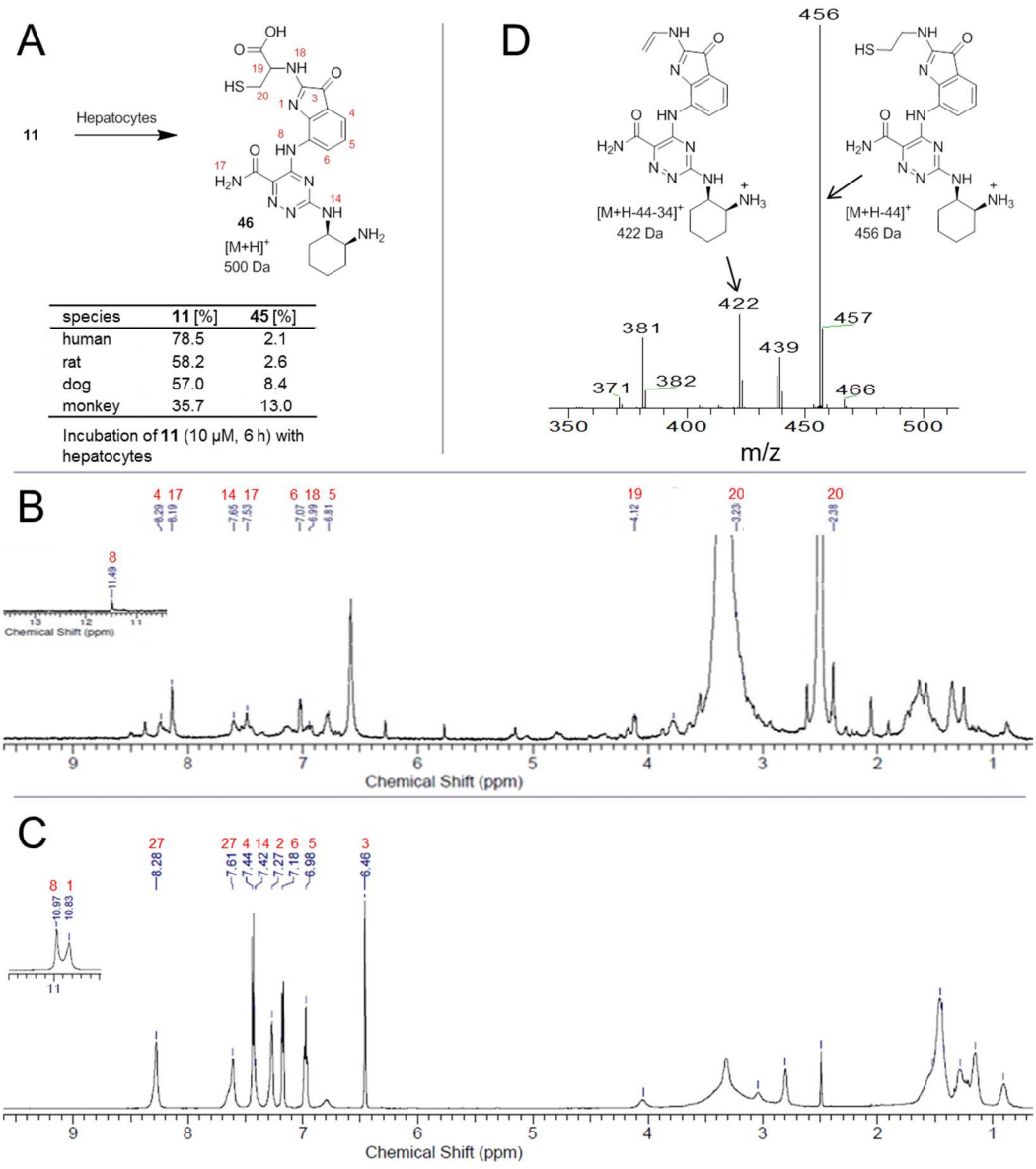

Figure 8. Metabolite **46**. (A) Formation in hepatocytes from different species. (B) ^{1}H-NMR spectrum of **46** and assignment of key signals (0.9 µg, DMSO-*d6*). (C) ^{1}H-NMR spectrum of **11** and assignment of key signals (DMSO-*d6*). Additional signals and broadening of signals due to

existence of different rotamers. (D) Collision-induced fragmentation of the protonated molecular ion of **46**.

CONCLUSIONS

We have described the discovery and characterization of the efficacious and selective Syk inhibitor **11**. Unfortunately, compound **11** could not be advanced to clinical trials because of liver findings in toxicology studies limiting the therapeutic index. However, we believe that compound **11** is a good tool compound to study the biology of Syk *in vitro* and *in vivo*.

EXPERIMENTAL SECTION

General. Reagents, solvents and heterocyclic building blocks (**14**, **21**, **26**, **30**, **34**, and **42**) were purchased from commercial sources and used without further purification. All reactions were carried out under an atmosphere of Argon. High-resolution LC/ESI-MS data were recorded using a Thermo Scientific LTQ Orbitrap XL mass spectrometer with an electrospray ionization source and a Shimadzu Nexera liquid chromatograph equipped with a diode array detector. The NMR spectra were obtained using a 400 MHz spectrometer. All ^{1}H NMR spectra are reported in δ units (ppm) and were recorded in DMSO-*d6* or CD_3OD and referenced to the solvent peaks. Liquid chromatography was performed on Acquity UPLC/MS systems (Waters, Milford, MA) equipped with a binary solvent manager, a sample manager, a column manager, a photodiode array detector (PDA) and a Waters ZQ2000 MS detector. Acquity UPLC columns (Waters, Milford, MA) with dimensions of 2.1x50 mm and packed with High Strength Silica (HSS) T3 particles of 1.8µ diameter and 100 Å pore size were used. The columns were housed at constant 60°C inside the column manager with a tolerance band of 0.1°C. The flow was 1 ml/min. The mobile phase

consisted of (A) water + 0.05% formic acid and (B) acetonitrile + 0.04% formic acid. The runtime was 2 min. The following gradient was used: from A/B 95:5→ 2:98 within 1.40 min; A/B 2:98 for 0.4 min; from A/B 2:98→95:5 within 0.1 min; A/B 95:5 for 0.1 min. UV absorption was monitored at λ = 210-450 nM. The MS detector was operated in continuously positive/negative ESI alternating mode with full scan from 120-1200 Da in 0.3 seconds. Mass spectra were acquired and stored in centroid mode. MS based confirmation of molecular weight was based on the formation of the pseudo-molecular ions $[M+H]^+$ in positive mode and $[M-H]^-$ in negative mode. All test compounds reported in this manuscript had a purity >95%.

Structure elucidation of 46: NMR spectra (^1H, ^{13}C, 2D ROESY (rotating frame nuclear Overhauser effect), HSQC (heteronuclear single quantum coherence) and HMBC (heteronuclear multiple bond correlation) were measured on a Bruker AVANCE III spectrometer (600 MHz proton frequency) equipped with a 1.7 mm $^1H\{^{13}C,^{15}N\}$ Bruker Biospin's TCI MicroCryoProbe™. ^1H and ^{13}C shifts were referenced internally to the solvent signals at 2.50 ppm and 39.5 ppm, respectively. Each metabolite sample was dissolved in about 40 µL DMSO-*d6* and transferred to a 1.7 mm NMR tube. MS investigations were performed on a LTQ XL Orbitrap (Linear Quadrupole 2D Ion Trap / Orbitrap, Thermo Scientific, CA, USA) mass spectrometer equipped with a captive spray ionization (CSI) source (Microchrom Bioresources, Auburn, USA) operating in positive mode electrospray ionization (ESI). The resolution was set to 30000 in full scan and 15000 in MS(n) mode. The omnipresent polysiloxane background ion $[C_2H_6SiO]_6$ with m/z 445.12003 was used as external lock mass.

16. LiHMDS (21.7 ml of 1M solution in THF, 21.7 mmol) was added at -78^{0}C to a solution of **15** (1193 mg, 7.45 mmol) in THF (15 ml) and the mixture stirred for 1 h. A solution of **14** (1300 mg, 6.77 mmol) in THF (5 ml) was added at -78^{0}C, the mixture warmed to 25^{0}C and stirred for 1 h.

The mixture was poured into ice cold 2 N HCl, extracted with CH_2Cl_2, dried with Na_2SO_4 and the solvent removed. The residue was crystallized from cyclohexane/ether to yield **16** as a light brown solid (1700 mg, 79%). UPLC retention time 1.09 min. ^{1}H-NMR DMSO-*d6* δ=13.9 (1 H, s), 10.78 (1 H, m), 8.53 (m, 1 H), 8.28 (1 H, d), 8.15 (2 H, s), 7.73 (m, 1 H), 7.64 (1 H, m), 7.54 (1 H, t), 7.00 (1 H, d). ES/ESI 316 $[M + H]^+$.

17. To a solution of **16** (1700 mg, 5.38 mmol) in DMF (10 ml) was added CDI (1528 mg, 9.45 mmol) and the mixture stirred for 16 h at 25^{0}C. Methanol (10 ml) was added within 10 min and stirring continued for 30 min. The mixture was poured into water and the precipitate filtered off. Compound **17** (1650 mg, 92%) was isolated as a brown solid. UPLC retention time 1.32 min. ^{1}H-NMR DMSO-*d6* δ=10.33 (1 H, m), 8.54 (m, 1 H), 8.29 (1 H, d), 8.14 (2 H, s), 7.74 (m, 1 H), 7.62 (1 H, m), 7.54 (1 H, t), 7.02 (1 H, d), 3.91 (3 H, s). ES/ESI 330 $[M + H]^+$.

19. A mixture of **17** (500 mg, 1.516 mmol), **18** (487 mg, 2.275 mmol) and DIPEA (588 mg, 4.55 mmol) in NMP (5 ml) was stirred for 16 h at 120^{0}C. The mixture was cooled to 25^{0}C, poured into water, extracted with ethyl acetate and the organic phase dried with Na_2SO_4. The solvent was removed and the residue purified by chromatography (ethyl acetate/cyclohexane gradient) to yield **19** (720 mg, 93%) as a yellow oil. UPLC retention time 1.42 min. ^{1}H-NMR DMSO-*d6* δ=10.65 (1 H, m), 8.84 (m, 1 H), 8.12 (2 H, s), 7.82 (m, 1 H), 7.63 (1 H, m), 7.47 (2 H, m), 7.12 (1 H, m), 6.42 (1 H, m), 6.11 (1 H, d), 4.31 (1 H, m), 3.83 (1 H, m), 3.80 (3 H, s), 1.78-1.05(8 H, m), 1.28 (9 H, s). ES/ESI 508 $[M + H]^+$.

20. A mixture of **19** (710 mg, 1.399 mmol), LiOH x H_20 (293 mg, 7 mmol), dioxane (4 ml) and water (1 ml) was stirred for 2 h at 100^{0}C. The mixture was cooled to 25^{0}C, water (50 ml) was added, the pH adjusted to 1 with 4N HCl, extracted with CH_2Cl_2. The organic phase was dried with Na_2SO_4 and the solvent removed to give 571 mg of the acid of **19** which was used without

further purification in the next step. UPLC retention time 1.21 min. ES/ESI 494 $[M + H]^+$. A mixture of the acid (250 mg, 0.507 mmol), DIPEA (72 mg, 0.557 mmol) and COMU (239 mg, 0.557 mmol) in DMF (3 ml) was stirred at 25^0C for 10 min, NH_4OH (10 mmol) was added and stirring continued for 1 h. The mixture was poured into aqueous $NaHCO_3$, extracted with ethyl acetate and the organic phase dried with Na_2SO_4. The solvent was removed and the residue purified by chromatography (ethyl acetate/cyclohexane gradient) to yield **20** (250 mg, 83% over 2 steps) as a yellow oil. UPLC retention time 1.15 min. ^{1}H-NMR DMSO-*d6* δ=12.05 (1 H, s), 8.76 (m, 1 H), 8.10 (2 H, s), 7.81 (1 H, m), 7.56 (1 H, m), 7.43 (2 H, m), 6.73 (1 H, m), 6.41 (1 H, m), 6.03 (1 H, d), 4.31 (1 H, m), 3.82 (1 H, m), 1.80-1.08(8 H, m), 1.28 (9 H, s). ES/ESI 493 $[M + H]^+$.

6. A mixture of **20** (250 mg, 0.508 mmol) and TFA (1157 mg, 10 mmol) in CH_2Cl_2 (2 ml) was stirred at 25^0C for 1 h. The solvent was removed and the residue purified by preparative HPLC. Product containing fractions were combined and passed through an Isolute SCX-2 column to yield the free base of **6** (70 mg, 35%) as a yellow solid. UPLC retention time 0.65 min. ^{1}H-NMR DMSO-*d6* δ=12.05 (1 H, s), 8.75 (m, 1 H), 8.10 (2 H, s), 7.80 (d, 1 H), 7.65 (1 H, m), 7.55 (1 H, m), 7.43 (2 H, m), 7.05 (1 H, m), 6.73 (1 H, m), 6.41 (1 H, m), 6.07 (1 H, d), 4.13 (1 H, m), 3.07 (1 H, m), 1.70-1.20 (8 H, m). HR-MS $[M + H]^+$ observed = 393.21469, estimated = 393.21458.

22. A mixture of **21** (1000 mg, 5.78 mmol), **18** (1363 mg, 6.36 mmol) and NEt_3 (702 mg, 6.94 mmol) in NMP (10 ml) was stirred at 75^0C for 16 h. The mixture was poured into ice water, the pH was adjusted to 1 with concentrated HCl and the precipitate collected. Chromatography (ethyl acetate/cyclohexane gradient) gave **22** (1200 mg, 59%) as a colorless solid. UPLC retention time 1.17 min. ^{1}H-NMR DMSO-*d6* δ=7.70 (m, 1 H), 7.46 (1 H, m), 6.61 (1 H, m), 6.27 (1 H, m), 4.10 (1 H, m), 3.77 (1 H, m), 1.72-1.25 (8 H, m), 1.33 (9 H, s). ES/ESI 351 $[M + H]^+$.

25. A mixture of **22** (500 mg, 1.425 mmol), 22 (226 mg, 1.71 mmol), $Pd(OAc)_2$ (19.2 mg, 0.086 mmol), Xantphos (99 mg, 0.172 mmol) and K_2CO_3 (2954 mg, 21.38 mmol) in dioxane (16 ml) was heated at 150^{0}C for 1.5 h. The mixture was diluted with ethyl acetate (40 ml) and washed with 0.1N HCl, saturated $NaHCO_3$ solution and brine. The organic phase was dried with Na_2SO_4, the solvent removed to give crude **24** (890 mg) which was used without purification for the next step. UPLC retention time 1.24 min. ES/ESI 447 $[M + H]^+$. A mixture of **24** (636 mg, 1.425 mmol) 4N NaOH (1.78 ml, 7.13 mmol), H_2O_2 (0.728 ml 30% solution), ethanol (8 ml) and DMSO (4 ml) was stirred at 25^{0}C for 3 h. The mixture was poured into water and extracted with saturated $NaHCO_3$ solution and brine. The organic phase was dried with Na_2SO_4, the solvent removed and the residue purified by chromatography (ethyl acetate/cyclohexane gradient) to yield **25** (500 mg, 73% over 2 steps) as a light brown solid. UPLC retention time 1.11 min. ^{1}H-NMR DMSO-*d6* δ=11.40 (1 H, s), 10.50 (1 H, s), 7.79 (1 H, d), 7.55 (1 H, m), 7.47 (1 H, d), 7.23 (3 H, m), 6.91 (1 H, t), 6.50 (1 H, m), 6.42 (1 H, m), 6.37 (1 H, m), 5.91 (1 H, d), 3.82 (1 H, m), 3.67 (1 H, m), 1.65-1.15 (8 H, m), 1.33 (9 H, s). ES/ESI 465 $[M + H]^+$.

7. At 0^{0}C 4N HCl in dioxane (5.27 ml, 21.1 mmol) was added to a solution of **25** (490 mg, 1.055 mmol) and CH_2Cl_2 (30 ml). The ice bath was removed and the mixture stirred for 2 h at 25^{0}C. Ethyl acetate was added and the mixture washed with $NaHCO_3$ solution and brine. The organic phase was dried with Na_2SO_4 and the solvent removed. The residue was purified by chromatography (ethyl acetate/methanol/NH_3 gradient) to give **7** (169 mg, 44%) as a colorless solid. UPLC retention time 0.61 min. ^{1}H-NMR DMSO-*d6* (100^{0}C; rotamers, not all NH signals visible) δ=10.70 (1 H, s), 10.18 (1 H, s), 7.81 (1 H, d), 7.42 (2 H, m), 7.28 (1 H, d), 7.20 (2 H, m), 6.93 (1 H, t), 6.42 (1 H, m), 6.01 (1 H, d), 3.82 (1 H, m), 3.19 (1 H, m), 1.72-1.15 (8 H, m). HR-MS $[M + H]^+$ observed = 365.20850, estimated = 365.20844.

27. At 0^0C a solution of **18** (2950 mg, 13.76 mmol) in DMF (5 ml) was added to a solution of **26** (2590 mg, 12.51 mmol) and NEt_3 (1267 mg, 12.51 mmol) in DMF (20 ml). The ice bath was removed and the mixture stirred for 16 h at 25^0C. The mixture was diluted with ethyl acetate and washed with water and brine. The organic phase was dried with Na_2SO_4 and the solvent removed. The residue was purified by chromatography (ethyl acetate/cyclohexane gradient) to give the regioisomer of **27** (950 mg, 19%) as a yellow solid and **27** (3460 mg, 71%) as a colorless solid. Regioisomer of **27**: UPLC retention time 1.21 min. ^{1}H-NMR DMSO-*d6* δ=8.28 (1 H, d), 7.89 (1 H, s), 6.93 (1 H, d), 4.27 (1 H, m), 3.84 (3 H, s), 3.81 (1 H, m), 1.68-1.15 (8 H, m), 1.31 (9 H, s). ES/ESI 385 $[M + H]^+$. **27**: UPLC retention time 1.03 min. ^{1}H-NMR DMSO-*d6* δ=7.98 (1 H, s), 7.90 (1 H, d), 6.70 (1 H, d), 4.15 (1 H, m), 3.77 (3 H, s), 3.75 (1 H, m), 1.70-1.15 (8 H, m), 1.32 (9 H, s). ES/ESI 385 $[M + H]^+$.

28. A mixture of **27** (300 mg, 0.780 mmol), **15** (187 mg, 1.169 mmol), $Pd(OAc)_2$ (1.8 mg, 0.008 mmol), Xantphos (9.0 mg, 0.016 mmol), K_2CO_3 (1077 mg, 7.89 mmol) and dioxane (2 ml) was heated at 90^0C for 16 h. The mixture was diluted with ethyl acetate and washed with 0.1N HCl, $NaHCO_3$ solution and brine. The organic phase was dried with Na_2SO_4 and the solvent removed. The residue was purified by chromatography (ethyl acetate/cyclohexane gradient) to give **28** (150 mg, 37%) as a colorless solid. UPLC retention time 1.23 min. ^{1}H-NMR DMSO-*d6* δ=10.60 (1 H, s), 8.82 (1 H, m), 8.11 (2 H, s), 7.72 (1 H, m), 7.68 (1 H, d), 7.56 (1 H, s), 7.51 (1 H, t), 7.41 (1 H, m), 6.60 (1 H, d), 4.25 (1 H, m), 3.90 (1 H, m), 3.82 (3 H, s), 1.79-1.05 (8 H, m), 1.31 (9 H, s). ES/ESI 509 $[M + H]^+$.

29. A mixture of 27 (150 mg, 0.295 mmol), LiOH x H2O (49.5 mg, 1.18 mmol), water (0.5 ml) and dioxane (1 ml) was stirred at 25^0C for 2 h. Ethyl acetate was added and the mixture washed with 0.1N HCl and brine. The organic phase was dried with Na_2SO_4 and the solvent removed to

give the acid of **27** which was used without purification for the next step. UPLC retention time 1.16 min. ES/ESI 495 $[M + H]^+$. DIPEA (36 mg, 0.279 mmol) and COMU (131 mg, 0.307 mmol) were added to a solution of the acid of **27** (138 mg) in DMF (2 ml) and the mixture stirred at 25^0C for 5 min. NH_3 (0.24 ml 25% aqueous solution, 6.14 mmol) and DIPEA (36 mg, 0.279 mmol) were added and the mixture was stirred at 25^0C for 30 min. The mixture was diluted with ethyl acetate, washed with saturated $NaHCO_3$ solution and brine. The organic phase was dried with Na_2SO_4 and the solvent removed to give **29** (117 mg, 80%) which was used without purification for the next step. UPLC retention time 1.17 min. ^{1}H-NMR DMSO-*d6* δ=11.75 (1 H, s), 8.80 (1 H, m), 8.10 (2 H, s), 7.77 (m, 1 H), 7.62 (1 H, d), 7.50-7.35 (4 H, m), 7.30 (1 H, m), 6.53 (1 H, m), 4.30 (1 H, m), 3.92 (1 H, m), 1.78-1.05 (8 H, m), 1.29 (9 H, s). ES/ESI 494 $[M + H]^+$.

8. A mixture of **29** (117 mg, 0.237 mmol), concentrated HCl (4.74 mmol), CH_2Cl_2 (10 ml) and methanol (1 ml) was stirred at 25^0C for 16 h. Ethyl acetate (20 ml) was added and the mixture washed with saturated $NaHCO_3$ solution. The organic phase was evaporated to a smaller volume and **8** precipitated by the addition of cyclohexane (74 mg of a light brown solid, 75 %). UPLC retention time 0.74 min. ^{1}H-NMR DMSO-*d6* δ=11.75 (1 H, s), 8.88 (1 H, m), 8.12 (2 H, s), 7.79 (m, 1 H), 7.62 (1 H, d), 7.55 (1 H, s), 7.54 (1 H, m), 7.48 (1 H, t), 7.35 (2 H, m), 4.21 (1 H, m), 3.84 (1 H, m), 3.20 (2 H, m), 1.78-1.25 (8 H, m). HR-MS $[M + H]^+$ observed = 394.20960, estimated = 394.20983.

31. At 0ºC **17** (739 mg) in DMF (2 ml) was added to a solution of **30** (500 mg) and NEt_3 (0.401 ml, 2.87 mmol) in DMF (5 ml) and the mixture stirred for 16 h at 25ºC. The mixture was diluted with ethyl acetate (50ml) and washed with water (50ml). The aqueous phase was extracted with ethyl acetate (30ml), the combined organic phases washed with brine, dried over Na_2SO_4 and the

solvent removed. Chromatography on silica (gradient cyclohexane/ethyl acetate) gave **31** (905 mg, 90 %) as a colorless solid. UPLC retention time 1.13 min. ^{1}H-NMR DMSO-*d6* δ=8.36 (1 H, m), 8.02 (1 H, s), 6.79 (1 H, d), 4.17 (1 H, m), 3.77 (1 H, m), 1.70-1.25 (8 H, m), 1.32 (9 H, s). ES/ESI 352 $[M + H]^+$.

32. To **31** (300 mg) in dioxane (2 ml) was added under argon **23** (135 mg), K_2CO_3 (1178 mg), $Pd(OAc)_2$ (1.91 mg) and Xantphos (9.9 mg,). The mixture was stirred for 16 h at 90°C. The mixture was diluted with ethyl acetate (20ml), washed with HCl (0.1N; 30ml). The aqueous phase was extracted with ethyl acetate (20ml), the combined organic phases washed with bicarbonate solution and brine, dried over Na_2SO_4 and the solvent removed. Chromatography on silica (gradient cyclohexane/ethyl acetate) gave **32** (368mg, 96 %). UPLC retention time 1.19 min. ES/ESI 448 $[M + H]^+$.

33. To **32** (368 mg) in DMSO (2 ml) and EtOH (4 ml) was added at 0°C 4N NaOH (1.03 ml) and H_2O_2 (0.382 ml). After stirring for 2 h at 25ºC the mixture was partitioned between water and ethyl acetate (30ml each). The organic phase was washed with bicarbonate solution and brine, dried over Na_2SO_4 and the solvent removed to give crude **32** (320mg) which was used without further purification in the next step. UPLC retention time 1.18 min. ^{1}H-NMR DMSO-*d6* δ=11.05 (1 H, s); 10.70 (1 H, m); 7.67 (1 H, m); 7.38 (2H, m); 7.30 (1 H, d); 7.23 (1 H, t); 7.20 (2 H, m); 6.50 (1 H, m); 6.43 (1 H, m); 3.75 (2 H, m); 1.65-1.05 (8 H, m), 1.31(9 H, s). ES/ESI 466 $[M + H]^+$.

9. To **33** (320 mg) in CH_2Cl_2 (20 ml) and MeOH (4 ml) was added 4H HCl (3.44 ml) and the mixture stirred for 16 h at 25ºC. The mixture was diluted with CH_2Cl_2 (50ml) and washed with bicarbonate solution and brine, dried with Na_2SO_4 and the solvent removed. Chromatography using a KP-NH column (gradient MeOH/ethyl acetate) gave **9** (74 mg, 29 %) as a yellow solid.

UPLC retention time 0.65 min. ^{1}H-NMR DMSO-*d6* δ=11.04 (1 H, s); 10.71 (1 H, s); 7.67 (1 H, m); 7.42 (1H, s); 7.32 (1 H, d); 7.28 (1 H, d); 7.24 (1 H, m); 7.22 (1 H, m); 7.18 (1 H, m); 6.93 (1 H, t); 6.44 (1 H, m); 3.65 (1 H, m); 2.87 (1 H, m); 1.55-1.03 (8 H, m). HR-MS $[M + H]^+$ observed = 366.20353, estimated = 366.20368.

35. Compound **15** (360 mg, 2.245 mmol) was added to a solution of **34** (500 mg, 2.140 mmol) in NMP (2.5 ml) at 0^{0}C, the cooling bath was removed and the mixture stirred for 30 min at 25^{0}C. The suspension was diluted with methanol (3.5 ml), the precipitate filtered off, washed with diethyl ether and dried to give **35** (608 mg, 78 %) as a beige solid. UPLC retention time 1.12 min. ^{1}H-NMR DMSO-*d6* δ=10.40 (1 H, s), 8.73 (1 H, m), 8.15 (2 H, s), 7.87 (1 H, m), 7.58 (2 H, m), 4.46 (2 H, q), 2.60 (3 H, s), 1.39 (3 H, t). ES/ESI 360 $[M + H]^+$.

36. A suspension of **35** (300 mg, 0.823 mmol) in NH_3/methanol (3 ml 7N solution) was stirred at 25^{0}C for 2 h. The mixture was poured into ice water, the precipitate filtered off, washed with water and dried to give **36** (254 mg, 92 %) as a beige solid. UPLC retention time 0.95 min. ^{1}H-NMR DMSO-*d6* δ=11.90 (1 H, s), 8.80 (2 H, m), 8.15 (3 H, m), 7.83 (1 H, d), 7.60 (1 H, t), 7.55 (1 H, d), 2.61 (3 H, s). ES/ESI 329 $[M + H]^+$.

37. To a suspension of **36** (250 mg, 0.746 mmol) in DMF (2.5 ml) was added at 0^{0}C *m*-CPBA (334 mg, 1.492 mmol), the ice bath was removed and the mixture stirred for 2 h at 45^{0}C. To the yellow suspension were added at 25^{0}C NEt_3 (385 mg, 3.81 mmol) and **18** (196 mg, 0.913 mmol). The mixture was stirred for 2 h at 65^{0}C. The mixture was concentrated and purified by preparative HPLC to give **37** (323 mg, 81 %) as a beige solid. UPLC retention time 1.03 min. ES/ESI 495 $[M + H]^+$.

10. A solution of **37** (323 mg, 0.655 mmol) and TFA (1.5 ml, 19.5 mmol) in CH_2Cl_2 (2 ml) was stirred at 25^{0}C for 1 h. The solvent was removed and the residue purified by preparative HPLC.

Product containing fractions were combined, the solvent removed and the residue dissolved in CH_2Cl_2. The organic phase was washed with 1N NaOH, dried over Na_2SO_4 and the solvent removed to give the free base **10** (130 mg, 49 %). UPLC retention time 0.64 min. ^{1}H-NMR DMSO-*d6* δ=11.70 (1 H, s), 8.92 (1H, s), 8.38 (1 H, s), 8.12 (2 H, s), 7.75 (3 H, m), 7.54 (1 H, t), 7.42 (1 H, m), 3.97 (1 H, m), 3.08 (1 H, m), 1.73-1.22 (8 H, m). HR-MS $[M + H]^+$ observed = 395.20486, estimated = 395.20508.

38. Compound **23** (283 mg, 2.140 mmol) was added to a solution of **34** (500 mg, 2.140 mmol) in NMP (2 mL) and the mixture stirred at 25ºC for 15 min. The mixture was added to water, the precipitate collected and dried to give compound **38** (660 mg, 84 %) as a beige solid. UPLC retention time 1.07 min. ^{1}H-NMR DMSO-*d6* δ=10.81 (1 H, s); 10.00 (1 H, s); 7.53 (1 H, d); 7.34 (1H, t); 7.11 (1 H, d); 7.03 (1 H, t); 6.49 (1 H, m); 4.49 (2 H, q); 2.01 (3 H, s); 1.41 (3 H, t). ES/ESI 330 $[M + H]^+$.

39. To a suspension of **38** (660 mg, 1.803 mmol) and DMAP (22.5 mg, 0.180 mmol) in THF (4 mL) was added at 0ºC a solution of $(Boc)_2O$ (437 mmg, 1.984 mmol) in THF (3 mL). The mixture was stirred at 25ºC for 30 min. The solvent was removed and the residue purified by chromatography on silica (gradient cyclohexane/ethyl acetate) to give compound **39** (555 mg, 70 %) as a yellow solid. UPLC retention time 1.28 min. ^{1}H-NMR DMSO-*d6* δ=10.50 (1 H, s); 7.67 (1 H, d); 7.61 (1H, d); 7.44 (1 H, d); 7.32 (1 H, t); 6.77 (1 H, d); 4.48 (2 H, q); 2.09 (3 H, s); 1.40 (3 H, t), 1.38 (9 H, s). ES/ESI 430 $[M + H]^+$.

40. A mixture of **39** (260 mg, 0.593 mmol) and NH_3 (2 mL of a 7 molar solution in methanol) was stirred at 25ºC for 45 min. The mixture was added to ice water, the precipitate collected and dried to give compound **40** (183 mg, 76 %). UPLC retention time 1.09 min. ^{1}H-NMR DMSO-*d6*

δ=11.50 (1 H, s); 8.67 (1 H, s), 8.05 (1 H, s), 7.68 (1 H, d); 7.61 (1H, d); 7.36 (1 H, d); 7.31 (1 H, t); 6.77 (1 H, d); 2.09 (3 H, s); 1.32 (9 H, s). ES/ESI 401 $[M + H]^+$.

41. To a solution of **40** (180 mg, 0.445 mmol) in DMF (2 mL) was added *m*-CPBA (199 mg, 0.890 mmol) at 0ºC and the mixture stirred for 45 min. NEt_3 (225 mg, 2.225 mmol) and **18** (95 mg, 0.445 mmol) were added and the mixture stirred at 65ºC for 15 min. The solvent was removed and the residue purified by preparative HPLC to give compound **41** (222 mg, 72 %) as a yellow solid. UPLC retention time 1.13 min. ES/ESI 567 $[M + H]^+$.

11. A solution of **41** (222 mg, 0.323 mmol) in CH_2Cl_2 (2 mL), TFA (2 mL) and water (0.02 mL) was stirred at 25ºC for 0.5 h. Then the mixture was kept for 16 h at 0ºC and for 1 h at 25ºC. The solvents were evaporated and the residue purified by preparative HPLC. The product was dissolved in CH_2Cl_2 and extracted with 1N NaOH to give **11** (62 mg) as a yellow solid. UPLC retention time 0.59 min. ^{1}H-NMR (400 MHz; CD_3OD): 7.59 (1 H, d); 7.30 (1 H, d); 7.18 (1 H, d); 7.09 (1 H, t); 6.58 (1 H, d); 3.70 (1 H, m); 3.20 (1 H, m); 1.80-1.30 (8 H, m). HR-MS $[M + H]^+$ observed = 367.19910, estimated = 367.19893.

12 (HCl salt)**.** UPLC retention time 0.52 min. ^{1}H-NMR (400 MHz; CD_3OD): 7.79 (1 H, d); 7.44 (1 H, d); 7.41 (1 H, d); 7.25 (1 H, t); 6.64 (1 H, d); 4.38 (1 H, m); 3.70 (1 H, m); 2.00-1.55 (8 H, m). ES/ESI 367 $[M + H]^+$. HR-MS $[M + H]^+$ observed = 367.19895, estimated = 367.19893.

45. A mixture of **42** (455 mg, 2.372 mmol), **23** (313 mg, 2.372 mmol) and NEt_3 (1392 mg, 13.76 mmol) in THF (30 ml) was stirred at 25^{0}C for 16 h. The solvent was removed and the residue extracted with ethyl acetate to give a grey solid (**43**) which was used without further purification in the next step. The solid was dissolved in DMF (7 ml), **44** (589 mg, 2.372 mmol) and NEt_3 (705 mg, 5.46 mmol) were added and the mixture was heated for 3 h at 110^{0}C. Ethyl acetate was added and the mixture washed with water and brine. The organic phase was dried over Na_2SO_4

and the solvent removed. The residue was purified by chromatography on silica (gradient cyclohexane/ethyl acetate) to give **45** (720 mg, 52 %) as a light brown solid. UPLC retention time 1.01 min. ES/ESI 500 $[M + H]^+$.

13. A mixture of **45** (360 mg, 0.62 mmol) and 10% Pd/C (75 mg, 0.07 mmol) in methanol (20 ml) was stirred for 3.5 h at 25^0C in the presence of an atmosphere of H_2 (balloon). The mixture was filtered through Hyflo, the solvent removed and the residue purified by preparative HPLC. Product containing fractions were combined and passed through an Isolute SCX-2 column to yield the free base of **13** (68 mg, 30%) as a yellow solid. UPLC retention time 0.59 min. ^{1}H-NMR (400 MHz; CD_3OD): 7.59 (1 H, d); 8.48 (1 H, s), 7.46 (1 H, d); 7.22 (1 H, d); 7.14 (1 H, d); 7.01 (1 H, t); 6.48 (1 H, d), 3.62 (1 H, m); 2.77 (1 H, m); 1.80-1.30 (8 H, m). ES/ESI 366 $[M + H]^+$. HR-MS $[M + H]^+$ observed = 366.20368, estimated = 366.20368.

Syk kinase assay. The assay was performed as endpoint determination using 384 well microtiter plates. Compounds were tested as 8-point dose responses. The assays were prepared by addition of 50nl compound solution in 90% DMSO directly into the empty plate using a hummingbird dispenser (Zinsser, Germany). Subsequently, 4.5µl of a mixture of 4µM ATP and 4µM peptide (5-Fluo-Ahx-GAPDYENLQELNKK-Amide) in reaction buffer (50mM HEPES, pH 7.5, 1mM DTT, 0.02% Tween20, 0.02% BSA, 0.6% DMSO, 10mM beta-glycerophosphate, and 10µM sodium orthovanadate, 1mM MgCl2, 3mM $MnCl_2$) were added to each well. The kinase reactions were started by further addition of 4.5µl of enzyme solution (4nM Syk (2-635) in reaction buffer). After 60min incubation at 30°C, reactions were terminated by addition of 16µl per well of EDTA stop solution. Product formation was measured in a microfluidic mobility shift assay (Caliper LC3000, Perkin Elmer).

Syk cellular assay. Ramos B cells were grown and passaged in RPMI 1640 medium (Gibco) containing 10 % FCS. On the day of the experiment cells were washed with serum free medium and dispensed into microtiter plates followed by addition of compound and incubated for 30 min at 37°C. The cells were then stimulated by addition of anti-IgM (Bioconcept, final concentration 20 µg/ml) for 15 min at 37°C. In each experiment 8-fold serial dilutions of compounds were tested. The stimulation was quenched by addition of 100 µl/well of formaldehyde (final conc. 2%) for 15min, followed by centrifugation: The cell pellet was resuspended in 100 µL 90% methanol and further incubated for 30 min at 4°C. The cells were then washed three times with 2% FCS in PBS. Phospho BLNK was assessed by flow cytometry using a FACSCalibur or a CyAn(Hypercyt) instrument using anti-BLNK (pY84)Mab-Alexa647 (BD Bioscience). Fluorescence values were evaluated in FlowJo followed by Excel / XLfit. The IC_{50} values were calculated by using a factor taking into account the mean fluorescence intensity (MFI) of P-BLNK-stained activated Ramos cells and the percentage of stained cells above a threshold set to exclude >99% of unstained cells. The factor is calculated according to the formula F=MFI * % positive cells.

Syk assay in human blood. Blood was collected from healthy volunteers by venipuncture into Monovette heparin tubes. The whole blood was dispensed into microtiter plate wells and compounds to be tested were added and incubated for 30 min at 37°C. Into a second plate 10µL pre warmed anti human CD32 (eBioscience, 10-fold concentrate; 50µg/ml final) was added. Then 100µl of blood + compound sample from the first plate was transferred to plate 2, mixed and incubated for 5 min at 37°C followed by red cell lysis in Lyse Fix (BD Bioscience). The plate was then centrifuged and the cell pellet permeabilized in 90% methanol and washed as described above. The cells were stained with anti CD14-Pacific Blue (eBioscience) to identify the

monocytes and anti-SLP76 (pY128)Mab-Alexa647 (BD Bioscience). The IC_{50} values for inhibition of P-SLP76 in CD14+ monocytes was assessed by flow cytometry as described above.

Mouse bone marrow cell proliferation assay. Serial dilutions of compound samples were prepared in 50 µl RPMI medium in a 96-well plate. Freshly isolated bone marrow cells of C57/Bl6 mice were adjusted to $5x10^5$/ml in RPMI containing WEHI and L929 conditioned medium (as a source of IL3) or recombinant IL-3 at appropriate concentrations. Fifty µl of the cell suspension ($2.5x10^4$ cells) were added to each well containing compounds. Cultures without any compound sample were used as high controls; cultures without compound or IL-3 were used as low controls. Cultures were incubated for 4 days at 37ºC in 5 % CO_2. One µCi ^{3}H-thymidine was added to each well and incubated for an additional 5 hours. Cells were then harvested with a Betaplate 96-well harvester on filter paper, the filter was washed, dried and counted after addition of scintillation liquid in a Betaplate counter.

Zap70 cellular assay. Jurkat T cells were washed twice with RPMI 1640 / 0.1% FCS and resuspended in the same medium. Compounds to be tested were dispended into wells of a microtiter plate (25µl compound solution 2-fold concentrated in RPMI + 0.1% FCS). Cells were added to the wells with compound ($2x10^5$ cells/25µL) and incubated for 30 min at 37˚C. Stimulation of the TCR was achieved by addition of 50µL/well of anti TCR antibody OKT3 (ACE10273, 30 µg/mL final concentration) diluted in pre-warmed medium and incubated for 2 min at 37˚C. The stimulation was stopped by addition of 100µl PFA/PBS (2% PFA final concentration) followed by incubation for 15 min at 37˚C. Cells were centrifuged and resuspended in 100µl methanol 90% and further incubated for 30min at 4˚ C. Permeabilized cells were washed once with PBS and then twice with 150µL/well FACS buffer (PBS + 2% FCS) and the last cell pellet was stained with anti-SLP76(pY128)Mab-Alexa647 (BD Bioscience) for 80

min at RT in the dark, washed and resuspend in 200µl FACS buffer and read on a FACS Calibur instrument. The IC_{50} values were calculated based on the Factor as described above for Ramos B cells.

Collagen induced arthritis and histology. Female Lewis rats (140-160g) were purchased from Janvier. Rats were kept under standard conditions (optimal health conditions [CHC], 22 ºC in special, acclimatized animal rooms with 12 h dark-light cycles, light from 0600 to 1800) with free access to tap water and pelleted rodent chow. The rats were allowed to acclimatize upon arrival at least for seven days before entering the study. This study was performed according to current Swiss animal protection laws issued by the Cantonal Veterinary Office Basel-Stadt, Switzerland. Freund's incomplete adjuvant (IFA, Difco, Detroit, USA) was mixed with porcine collagen type II (Chondrex, Redmond, USA) using a polytron on ice. The final solution consisted of 200 µg of collagen in 200 µl of IFA. Two hundred µl of this was injected intradermally (i.d.) into the base of the tail of an isofluorane narcotisized rat. After 7 days, the animal was boosted i.d. with a fresh batch of the immunization solution; (this time 100 µg in 100 µl) in an adjacent site at the base of the tail. When sufficient animals had developed arthritis, they were randomized into groups of 6 or 7 so that they all had the same average swelling score. This was on day 15 after initial immunization. At this time 300 µl heparin blood was taken for baseline PD assessment. Compound was diluted in 0.5% CMC/0.5% Tween 80 in water and was applied p.o. at a dose of 3, 10 and 30 mg/kg q.d. Compound was applied in a therapeutic setting starting at day 15 and continued until day 28. Swelling was scored 3 times a week. On days 19 and 20 300 µl heparin blood was taken at trough (24h) and at 4h (peak) for PD, and 100µl EDTA blood taken at 4h, 8h and 24h, for PK analysis. On day 28, animals were sacrificed and hind paws taken for histopathological analysis. Animals were weighed regularly throughout the study. Mean values of group were calculated. Scoring of the hind paw swelling was done on a composite scale of 0-12

per rat, evaluating each paw by visual inspection in the metatarsal region with score 0-3 and in the ankle with score 0-3, thus obtaining maximally score 6 per paw. The paw scores were summed up to obtain a score for each individual animal. The individual sum scores of all the animals were averaged and SEMs were calculated. The scoring system used was: 0 = no detectable sign of inflammation; 1 = light swollen region; 2 = more obviously swollen region; 3 = ankylosis or severely swollen region. Hind paws samples were fixed in 10 % buffered formalin for 48 hours, decalcified over 16 days in Immunocal (Decal Chemical Corp., Tallman, USA) changed every 3-4 days, processed and embedded in paraffin (Paraplast Tissue Embedding Medium): Leica Microsystems,). Three-µm thick sections were stained with Giemsa and safranin O. Histopathological changes were blindly scored on a scale of 0 (normal) to 3 (severe changes). Following parameters were assessed: inflammatory cell infiltrates, joint damage and proteoglycan loss. Statistical analysis: Statistics for paw swelling, body weight and histopathological assessment were performed with a Dunnet's multiple comparisons test (1 way ANOVA).

Incubation of 11 with monkey liver slices: Animal experiments were performed in accordance with Swiss Animal Welfare regulations. Freshly excised liver was collected from an animal after euthanasia. All tissue slice experiments were carried out using Williams medium E supplemented with fetal bovine serum (10%), glucose (27 mM), insulin (1 µM), hydrocortisone (100 µM), methionine (500 µM), gentamycin (100 µM) and amphotericin B (3 µM). Stock solutions of test compounds (2 mM) were prepared in DMSO. Tissue cores (8 mm) from freshly excised liver were prepared using a tissue-coring tool. Slices of 230 µm thickness were prepared from the cores using a MD6000 Krumdieck live tissue microtome (Alabama Research and Development, Munford, AL, USA), filled with ice-cold medium under bubbling of O_2 and CO_2. After preparation, slices were washed and kept on ice in medium until use. Liver slices (4 per incubation vessel) were pre-incubated for 1 h at 37°C in 2 mL of medium under an atmosphere of

75% O_2, 5% CO_2, 20% N_2; 98% humidity in a rotating culture (4 rotations/min) in a HERAcell 240i incubator (Thermo Fischer Scientific, Waltham, MA, USA). Subsequently, the test compound (10 or 20 μM) was added, and the slices were incubated for a further 8 or 18 h. At the end of the incubation time, each incubation sample was quenched with 2 mL cold acetonitrile (4 ºC) and the mixture was frozen at -80 ºC until workup.

ASSOCIATED CONTENT

Accession Codes. The coordinates for the structures of **1** and **10** and **11** bound to the kinase domain of Syk have been deposited in the RCSB Protein Data Bank under PDB ID 4RX9, PDB ID 4RX7 and PDB IC 4RX8, respectively.

AUTHOR INFORMATION

*G.T. Tel: +41 61 3243342. Fax: +41 61 3246735. *E-mail:* gebhard.thoma@novartis.com

ACKNOWLEDGEMENTS

We gratefully acknowledge the expert assistance of Valerie Caballero, Thierry Délémonté, Ralf Endres, Werner Gertsch, Stephanie Harlfinger, Alice Hauchard, Dorothee Lehmann, Alexandre Luneau, Jürg Peter, Marc Schäfer, Tanja Senn, Phuoc Thanh Thai, and Grazyna Wieczorek.

ABBREVIATIONS

BCR, B-cell receptor; BLNK, B cell linker protein; CDI, carbonyldiimidazole; COMU, (1-Cyano-2-ethoxy-2-oxoethylidenaminooxy)dimethylamino-morpholino-carbenium

hexafluorophosphate; DIPEA, N,N-diisopropylethylamine; DMAP, 4-dimethylaminopyridine; DMF, dimethylformamide; GLP, good laboratory practice; hERG, human *Ether-à-go-go* Related Gene; ITAM, immunotyrosine activating motif; LiHMDS, lithium hexamethyldisilazide; MAPK, mitogen-activated protein kinase; *m*-CPBA, meta-chloroperoxybenzoic acid; NMP, *N*-Methyl-2-pyrrolidone; NFκB, nuclear factor 'kappa-light-chain-enhancer' of activated B-cells; PI3-kinase, phosphoinositide-3 kinase; PK, pharmacokinetics ; PKC, protein kinase C; PLCγ2a, phospholipase C-γ2a; SH2, Src 2; SEM, standard error of the mean; SLP65, Src homology 2 domain-containing leukocyte-specific phosphoprotein of 65 kDa; SLP76, SH2 domain containing leukocyte protein of 76 kDa; Syk, spleen tyrosine kinase; TFA, trifluoroacetic acid; UPLC, ultra performance liquid chromatography; Xantphos, 4,5-Bis(diphenylphosphino)-9,9-dimethylxanthene; ZAP70, zeta-chain-associated protein kinase.

REFERENCES

1. (a) Mócsai, A.; Ruland, J.; Tybulewicz, V. L. J. The SYK tyrosine kinase: a crucial player in diverse biological functions. *Nat. Rev. Immunol*. **2010**, *10*, 387-402; (b) Kulathu, Y.; Grothe, G.; Reth, M. Autoinhibition and adapter function of Syk. *Immunol. Rev.* **2009**, *232*, 286-299; (c) Gilfillan, A. M.; Rivera, J. The tyrosine kinase network regulating mast cell activation. *Immunol. Rev.* **2009**, *228*, 149-169; (d) Geahlen, R. L. Syk and pTyr'd: Signaling through the B cell antigen receptor. *Biochimica et biophysica acta* **2009**, *1793*, 1115-1127; (e) Koretzky, G. A.; Abtahian, F. Silverman, M. A. *Nat. Rev. Immunol.* **2006**, *6*, 67-78.

2. (a) Bajpai, M.; Chopra, P.; Dastidar, S. G.; Ray, A. Spleen tyrosine kinase : a novel target for therapeutic intervention of rheumatoid. *Expert Opi. Investig. Drugs*, **2008**, *17*, 641-

659; (b) Siraganian, R. P.; Zhang, J.; Suzuki, K.; Sada, K. Protein tyrosine kinase Syk in mast cell signaling. *Mol. Immunol.* **2002**, *38*, 1229-1233; (c) Wong, B. R.; Grossbard, E. B.; Payan, D. G.; Masuda, E. S. Targeting Syk as a treatment for allergic and autoimmune disorders. *Expert Opi. Invest. Drugs* **2004**, *13*, 743-763; (d) Ghosh, D.; Tsokos, G. C. Spleen tyrosine kinase: an Src family of non-receptor kinase has multiple functions and represents a valuable therapeutic target in the treatment of autoimmune and inflammatory diseases. *Autoimmunity*, **2010**, *43*, 48-55.

3. Geahlen, R. L. Getting Syk: spleen tyrosine kinase as a therapeutic target. *Trends Pharm. Sci.* **2014**, *35*, 414-422.

4. Taniguchi, T.; Kobayashi, T.; Kondo, J.; T., Kazuhiro; Nakamura, H.; Suzuki, J.; Nagai, K.; Yamada, T.; Nakamura, S.; Yamamura, H. Molecular cloning of a porcine gene syk that encodes a 72-kDa protein-tyrosine kinase showing high susceptibility to proteolysis. *J. Bio. Chem.* **1991**, *266*, 15790-15796.

5. (a) Singh, R.; Masuda, E. S.; Payan, D. G. Discovery and Development of Spleen Tyrosine Kinase (SYK) Inhibitors. *J. Med. Chem.* **2012**, *55*, 3614-3643; (b) Moore, W. J.; Richard, D.; Thorarensen, A. An analysis of the diaminopyrimidine patent estates describing spleen tyrosine kinase inhibitors by Rigel and Portola. *Expert Opin. Ther. Patents* **2010**, *20*, 1703; (c) Norman, P. Spleen tyrosine kinase inhibitors: a review of the patent literature 2010 - 2013. *Expert Opin. Ther. Patents* **2014**, *24*, 573-595; (d) Castillo, M.; Forns, P.; Erra, M.; Mir, M.; Lopez, M.; Maldonado, M.; Orellana, A.; Carreno, C.; Ramis, I.; Miralpeix, M.; Vidal, B. Highly potent aminopyridines as Syk kinase inhibitors. *Bioorg. Med. Chem. Lett.* **2012**, *22*, 5419-5423; (e) Forns, P.; Esteve, C.; Taboada, L.; Alonso, J. A.; Orellana, A.; Maldonado, M.; Carreno, C.; Ramis, I.; Lopez, M.; Miralpeix,

M.; Vidal, B. Pyrazine-based Syk kinase inhibitors. *Bioorg. Med. Chem. Lett.* **2012**, *22*, 2784-2788; (f) Lucas, M. C.; Goldstein, D. M.; Hermann, J. C.; Kuglstatter, A.; Liu, W.; Luk, K. C.; Padilla, F.; Slade, M.; Villasenor, A. G.; Wanner, J.; Xie, W.; Zhang, X.; Liao, C. Rational Design of Highly Selective Spleen Tyrosine Kinase Inhibitors. *J. Med. Chem.* **2012**, *55*, 10414-10423; (g) Padilla, F.; Bhagirath, N.; Chen, S.; Chiao, E.; Goldstein, D. M.; Hermann, J. C.; Hsu, J.; Kennedy-Smith, J. J.; Kuglstatter, A.; Liao, C.; Liu, W.; Lowrie, L. E., Jr.; Luk, K. C.; Lynch, S. M.; Menke, J.; Niu, L.; Owens, T. D.; O-Yang, C.; Railkar, A.; Schoenfeld, R. C.; Slade, M.; Steiner, S.; Tan, Y.-C.; Villasenor, A. G.; Wang, C.; Wanner, J.; Xie, W.; Xu, D.; Zhang, X.; Zhou, M.; Lucas, M. C. Pyrrolopyrazines as selective spleen tyrosine kinase inhibitors. *J. Med. Chem.* **2013**, *56*, 1677-1692; (h) Lucas, M. C.; Bhagirath, N.; Chiao, E.; Goldstein, D. M.; Hermann, J.; Hsu, P.-Y.; Kirchner, S.; Kennedy-Smith, J.: Kuglstatter, A.; Lukacs, C.; Menke, J.; Niu, L.; Padilla, F.; Peng, Y.; Polonchuk, L.; Railkar, A.; Slade, M.; Soth, M.; Xu, D.; Yadava, P.; Yee, C.; Zhou, M.; Liao, C. Using ovality to predict non-mutagenic, orally efficacious pyridazine amides as cell specific spleen tyrosine kinase inhibitors. *J. Med. Chem.* **2014**, *57*, 2683-2691; (i) Liddle, J.; Atkinson, F. L.; Barker, M. D.; Carter, P. S.; Curtis, N. R.; Davis, R. P.; Douault, C.; Dickson, M. C.; Elwes, D.; Garton, N. S.; Gray, M.; Hayhow, T. G.; Hobbs, C. I.; Jones, E.; Leach, S.; Leavens, K.; Lewis, H. D.; McCleary, S.; Neu, M.; Patel, V. K.; Preston, A. G. S.; Ramirez-Molina, C.; Shipley, T. J.; Skone, P. A.; Smithers, N.; Somers, D. O.; Walker, A. L.; Watson, R. J.; Weingarten, G. G. Discovery of GSK143, a highly potent, selective and orally efficacious spleen tyrosine kinase inhibitor. *Bioorg. Med. Chem. Lett.* **2011**, *21*, 6188-6194; (j) Moy, L. Y.; Jia, Y.; Caniga, M.; Lieber, G.; Gil, M.; Fernandez, X.; Sirkowski, E.; Miller, R.; Alexander, J. P.; Lee, H.-H.; Shin, J. D.; Ellis, J. M.; Chen, H.; Wilhelm, A.; Yu, H.; Vincent, S.; Chapman, R.

W.; Kelly, N.; Hickey, E.; Abraham, W. M.; Northrup, A.; Miller, T.; Houshyar, H.; Crackower, M. A. Inhibition of Spleen Tyrosine Kinase Attenuates Allergen-Mediated Airway Constriction. *Am. J. Respir. Cell Mol. Biol.* **2013**, *49*, 1085; (k) Luca, M. C.; Tan, S.-L. Small-molecule inhibitors of spleen tyrosine kinase as therapeutic agents for immune disorders: will promise meet expectations? *Future Med. Chem.* **2014**, *6*, 1811-1827.

6. Coffey, G.; DeGuzman, F.; Inagaki, M.; Pak, Y.; Delaney, S. M.; Ives, D.; Betz, A.; Jia, Z. J.; Pandey, A.; Baker, D.; Hollenbach, S. J.; Phillips, D. R.; Uma Sinha, U. Specific inhibition of spleen tyrosine kinase suppresses leukocyte immune function and inflammation in animal models of rheumatoid arthritis. *J. Pharm. Exp. Ther.* **2012**, *340*, 350-359.

7. http://www.clinicaltrials.gov/ct2/show/NCT01652937?term=biib-057&rank=1

8. (a) Golden, A. P.; Li, N.; Chen, Q.; Lee, T.; Nevill, T.; Cao, X.; Johnson, J.; Erdemli, G.; Ionescu-Zanetti, C.; Urban, L.; Holmqvist, M. IonFlux: A Microfluidic Patch Clamp System Evaluated with Human Ether-a-go-go Related Gene Channel Physiology and Pharmacology. *Assay Drug Dev. Technol.* **2011**, *9*, 608-619.

9. ICH S7B: The non-clinical evaluation of the potential for delayed ventricular repolarization (QT interval prolongation) by human pharmaceuticals, **2005**. http://www.ich.org/fileadmin/Public_Web_Site/ICH_Products/Guidelines/Safety/S7B/Step4/S7B_Guideline.pdf

10. Currie, K. S.; Kropf, J. E.; Lee, T.; Blomgren, P.; Xu, J.; Zhao, Z.; Gallion, S.; Whitney, J. A.; Maclin, D.; Lansdon, E. B.; Maciejewski, P.; Rossi, A. M.; Rong, H.; Macaluso, J.;

Barbosa, J.; Di Paolo, J. A.; Mitchell, S. A. Discovery of GS-9973, a Selective and Orally Efficacious Inhibitor of Spleen Tyrosine Kinase. *J. Med. Chem.* **2014**, *57*, 3856-3873.

11. Thoma, G.; Blanz, J.; Buhlmayer, P.; Druckes, P.; Kittelmann, M.; Smith, A. B.; van Eis, M.; Vangrevelinghe, E.; Zerwes, H.-G.; Che, J.; He, X.; Jin, Y.; Lee, C. C.; Michellys, P.-Y.; Uno, T.; Liu, H. Syk inhibitors with high potency in presence of blood. *Bioorg. Med. Chem. Lett.* **2014**, *24*, 2278-2282.

12. Jaguar software was used for DFT/B3LYP calculations in gas phase with the 6-311++G** basis set. Jaguar is a high- performance ab initio package for both gas and solution phase simulations. Bochevarov, A. D.; Harder, E.; Hughes, T. F.; Greenwood, J. R.; Braden, D. A.; Philipp, D. M.; Rinaldo, D.; Halls, M. D.; Zhang, J.; Friesner, R. A. Jaguar: A high-performance quantum chemistry software program with strengths in life and materials sciences. *Int. J. Quantum Chem.* **2013**, *113*, 2110-2142.

13. It is worthwhile to mention that the pyrimidine analog of **12** also showed a very limited oral bioavailability of 4%.

14. Compound **11** was assessed in the KINOMEscan screening platform which employs an active site-directed competition binding assay to quantitatively measure interactions between test compounds and kinases. These assays do not require ATP and thereby report thermodynamic interaction affinities, as opposed to IC_{50} values, which can depend on the ATP concentration. See: http://www.discoverx.com/services/drug-discovery-development-services/kinase-profiling/kinomescan

15. Williams, R. O. Collagen-induced arthritis as a model for rheumatoid arthritis. *Methods Mol. Med.* **2004**, *98*, 207-216.

Table of Contents Graphic.

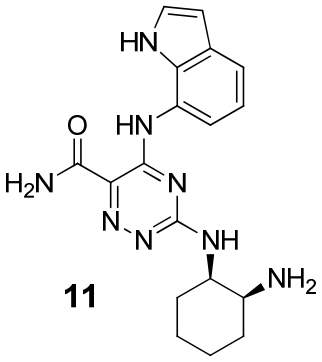

11

Syk (enzyme):	35 nM
Syk (cell):	99 nM
Syk (blood):	367 nM